

# **DESIGN, FABRICATION AND INSTALLATION OF A MICRO-HYDRO POWER PLANT**

**BY**

**OBAID ZIA**

**OSAMA ABDUL GHANI**

**SYED TALHA WASIF**

**ZOHAIB HAMID**

**Faculty of Mechanical Engineering  
GIK Institute of Engineering Sciences & Technology**

**MAY 2010**

## **ABSTRACT**

The total installed capacity of the hydropower stations in Pakistan is about 7,000 MW which is about 20% of the total available hydro power potential. For possible micro-hydro stations, a potential of about 1300 MW exists at a number of low head and high flow rate sites. In terms of turbine selection, there are a number of possibilities to exploit this potential. Considering the existing indigenous manufacturing expertise, Cross-Flow Hydraulic Turbines are the most feasible alternative in Pakistan. The aim of this project was to improve the existing design of the CFHTs that are being designed and installed in Pakistan. In order to accomplish this, extensive literature research has been carried out and the best design practices have been incorporated to reach a standard design for CFHTs with efficiencies reaching up to 70-80%. Besides design parameters, turbine design software and a comprehensive turbine manufacturing plan has been developed to facilitate the local manufacturers. The “MicroHydro Design Software” is an interactive tool that requires site data as input and calculates the appropriate turbine design parameters. In addition to the runner design, there are a few more considerations that are essential for a micro-hydro scheme to operate efficiently which include penstock design, power transmission mechanism design and generator selection. These are also included in the scope of the project and have been addressed in detail.

## **ACKNOWLEDGEMENTS**

We would like to extend our gratitude to Prof. Dr. Javed Ahmad Chattha, Dean FME and our FYP advisor for his help and support. We would also like to thank Dr. Muhammad Sultan Khan for his guidance.

We further wish to thank the manufacturer, Gukzar Khan, owner of Chiragh Engineering Works for his cooperation and help in fabricating the new design of Cross Flow Turbine.

## TABLE OF CONTENTS

Acknowledgements.....	iii
Table of Contents.....	iv
List of Tables.....	vii
List of Figures.....	viii
Nomenclature.....	ix
Chapter 1.....	1
Introduction.....	1
1.1 Need Statement.....	1
1.2 Background.....	1
1.3 Classification of Turbines.....	1
1.3.1 Reaction Principle: .....	1
1.3.2 Impulse Principle:.....	4
Chapter 2.....	7
Literature Review.....	7
Chapter 3.....	10
Turbine Design Parameters.....	10
3.1 Site Data.....	10
3.2 Theoretical Power Output.....	10
3.3 Runner Outer Diameter.....	10
3.4 Length of the Turbine Runner.....	12
3.5 Runner Inner Diameter.....	13
3.6 Thickness of Water Jet.....	13
3.7 Spacing of Blades.....	13
3.8 Number of Blades.....	13
3.9 Radius of Blade Curvature.....	14
3.10 Distance of Jet From Center of Shaft & Inner Periphery.....	14

3.10.1 Distance of jet from centre of shaft:.....	14
3.10.2 Distance of jet from inner periphery of the runner:.....	14
3.11 Angle of Attack.....	14
3.12 Angle between relative velocity of entering water jet and outer runner periphery ( $\beta_1$ ): .....	14
3.13 First Stage Blade Exit Angle ( $\beta_2'$ ).....	15
3.14 Runner Material.....	16
Chapter 4.....	17
Peripheral equipments.....	17
4.1 Penstock Design:.....	17
4.2 Power Transmission.....	19
4.3 Shaft Design.....	21
4.3.1 Shaft Deflection.....	22
Chapter 5.....	24
CAD Models FOR MANUFACTURING.....	24
5.1 Side Plates:.....	24
5.2 Runner Blade:.....	28
5.3 Runner Shaft:.....	29
Chapter 6.....	31
Software.....	31
Chapter 7.....	36
Conclusion.....	36
References.....	37
Appendix A.....	38
Technical Paper for Asme Power 2010 Conference, Chicago, IL, USA (July 13-15).....	38
Appendix B1.....	46
Software Code.....	46
1.Input Form Code.....	46
2.Results Page Code.....	49
3.Main Program Code.....	52
Appendix B2.....	54

Software Help File.....54

## LIST OF TABLES

Table 1 - Material Properties for Penstock Design.....	17
Table 2 - Weighted Index, Welded Steel.....	18
Table 3- Weighted Index, Cast Iron.....	18
Table 4 - Weighted Index, Ductile Iron.....	18

## LIST OF FIGURES

Figure 1 - Francis Turbine.....	2
Figure 2 - Kaplan Turbine.....	3
Figure 3 - Pelton Turbine.....	4
Figure 4 - Turgo Turbine.....	5
Figure 5 - Angle between relative velocity of entering water jet and outer runner periphery.	15
Figure 6 – First Stage Blade Exit Angles.....	15
Figure 7 - Belt Selection Envelopes (Fenner Wedge Belt Catalogue).....	20
Figure 8 - Runner Shaft Arrangement.....	22
Figure 9 - Shaft Deflection.....	23
Figure 10 - Side Disk CAD Model.....	28
Figure 11 - Runner Blade Dimensioning.....	29
Figure 12 - Runner Shaft.....	29
Figure 13 - Complete Runner Assembly.....	30
Figure 14 - Complete Turbine Assembly.....	31
Figure 15 - Input Form.....	33
Figure 16 - Output (SI Units).....	34
Figure 17 - Output (English Units).....	35



## NOMENCLATURE

**a** - Radial Rim Width

**C** - Coefficient accounting for nozzle roughness

**D<sub>2</sub>** - Inner Diameter of the runner

**d<sub>1</sub>** - Penstock Pipe diameter

**H** - Head

**h<sub>2</sub>** - vertical distance between 1<sup>st</sup> stage inlet and 2<sup>nd</sup> stage exit

**HP<sub>out</sub>** - Output Horse Power

**N** - Angular speed of the runner

**n** - Number of blades

**P<sub>t</sub>** - Theoretical Power Output

**Q** - Flow Rate

**S<sub>0</sub>** - Thickness of jet

**s<sub>1</sub>** - Tangential blade spacing

**t** - Blade spacing

**u<sub>1</sub>** - Tangential velocity of runner outer periphery

**u<sub>1</sub>'** - tangential velocity of runner inner periphery

**V** - Absolute velocity of water along the channel

**V<sub>1</sub>** - Absolute velocity of the entering water jet

**V<sub>1</sub>'** - Absolute velocity of entering water jet (2<sup>nd</sup> stage)

$V_2'$  - Absolute velocity of water from first stage exit

$v_1$  - relative velocity of the entering water jet

$v_1'$  - relative velocity of the entering water jet (2<sup>nd</sup> stage)

$v_2'$  - relative velocity of the water from first stage exit

$y_1$  - Distance of jet from centre of the shaft

$y_2$  - Distance of jet from inner periphery of the runner

### **Greek symbols**

$\alpha_1$  - angle of attack

$\alpha_2'$  - Angle between runner inner periphery and absolute velocity exiting water jet (1<sup>st</sup> stage)

$\beta_1'$  - angle between runner inner periphery and relative velocity of entering water jet (2<sup>nd</sup> stage)

$\beta_2'$  - angle between runner inner periphery and relative velocity of exiting water jet (1<sup>st</sup> stage)

$\alpha_1'$  - Angle between runner inner periphery and absolute velocity of entering water jet (2<sup>nd</sup> stage)

$\eta$  - Assumed System Efficiency

$\gamma$  - Specific weight of water

$\psi$  - Coefficient accounting for blade roughness

$\rho$  - Radius of blades curvature

# Chapter 1

## INTRODUCTION

### 1.1 Need Statement

The objective of this project is to design, fabricate and install a micro-hydro power plant for a chosen site in Mansehra, Khyber Pakhtunkhwa, Pakistan.

### 1.2 Background

Pakistan is going through its worst energy crisis due to the rapid depletion of fossil fuels. A staggering figure of 6000MW power deficiency has rendered the country handicapped in the economic and political domains, the evidence of which can be witnessed in forms of frequent industry shutdowns and furious public demonstrations. Pakistan is blessed with a rich hydropower potential, out of which only 20% is being exploited. Besides being the cheapest source of energy among the conventional energy generation methods, hydropower is 100% environment-friendly. It is imperative to make full use of this hydropower potential in order to meet the country's ever-growing energy demands. Significant proportion of this potential can be utilized with the use of micro-hydro schemes. A variety of turbines can be used for such micro-hydro schemes, depending upon the site characteristics. In Pakistan, Cross-Flow Hydraulic Turbine is the most widely used turbine for micro-hydro power plants. Its efficiency, convenient manufacturing and cheap maintenance make it an attractive choice for the manufacturers as well as investors.

### 1.3 Classification of Turbines

The potential energy in the water is converted into mechanical energy in the turbine, by one of two fundamental and basically different mechanisms:

#### 1.3.1 Reaction Principle:

The water pressure can apply a force on the face of the runner blades, which decreases as it proceeds through the turbine. Turbines that operate in this way are called reaction turbines. The turbine casing, with the runner fully immersed in water, must be strong enough to withstand the operating pressure.

**Francis turbines:**

Francis turbines are radial flow reaction turbines, with fixed runner blades and adjustable guide vanes, used for medium heads. In the high speed Francis the admission is always radial but the outlet is axial. The water proceeds through the turbine as if it was enclosed in a closed conduit pipe, moving from a fixed component, the distributor, to a moving one, the runner, without being at any time in contact with the atmosphere. It should be emphasized that the size of the spiral casing contrasts with the lightness of a Pelton casing. The wicket gates can be used to shut off the flow to the turbine in emergency situations, although their use does not preclude the installation of a butterfly valve at the entrance to the turbine. Francis turbines can be set in an open flume or attached to a penstock. Steel spiral casings are used for higher heads, designing the casing so that the tangential velocity of the water is constant along the consecutive sections around the circumference; this implies a changing cross-sectional area of the casing. Small runners are usually made in aluminum bronze castings. Large runners are fabricated from curved stainless steel plates, welded to a cast steel hub.

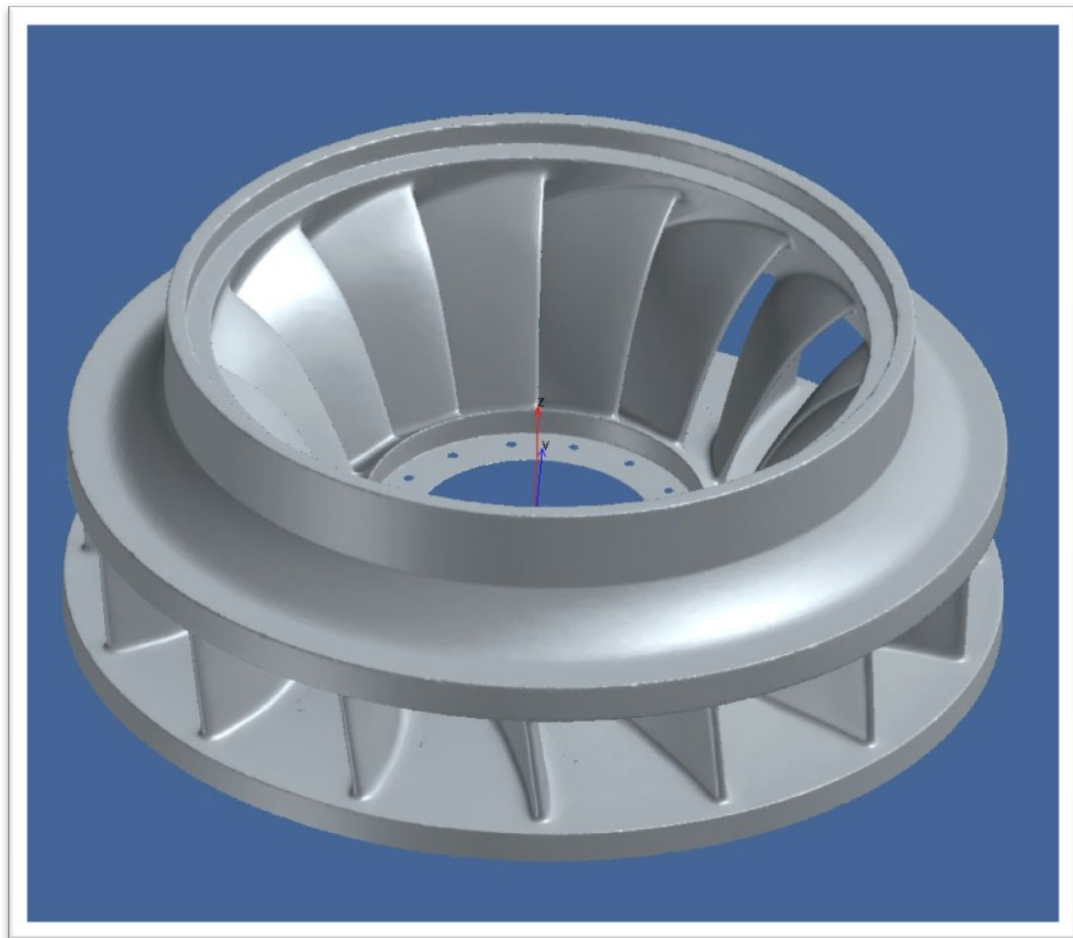


**Figure 1 - Francis Turbine**

### **Kaplan and propeller turbines:**

Kaplan and propeller turbines are axial-flow reaction turbines, generally used for low heads. The Kaplan turbine has adjustable runner blades and may or may not have adjustable guide-vanes. If both blades and guide-vanes are adjustable it is described as .double-regulated. If the guide-vanes are fixed it is .single-regulated. Unregulated propeller turbines are used when both flow and head remain practically constant. The double-regulated Kaplan is a vertical axis machine with a scroll case and a radial wicket-gate configuration. The flow enters radially inward and makes a right angle turn before entering the runner in an axial direction. The control system is designed so that the variation in blade angle is coupled with the guide-vanes setting in order to obtain the best efficiency over a wide range of flows. The blades can rotate with the turbine in operation, through links connected to a vertical rod sliding inside the hollow turbine axis.

Bulb units are derived from Kaplan turbines, with the generator contained in a waterproofed bulb submerged in the flow.

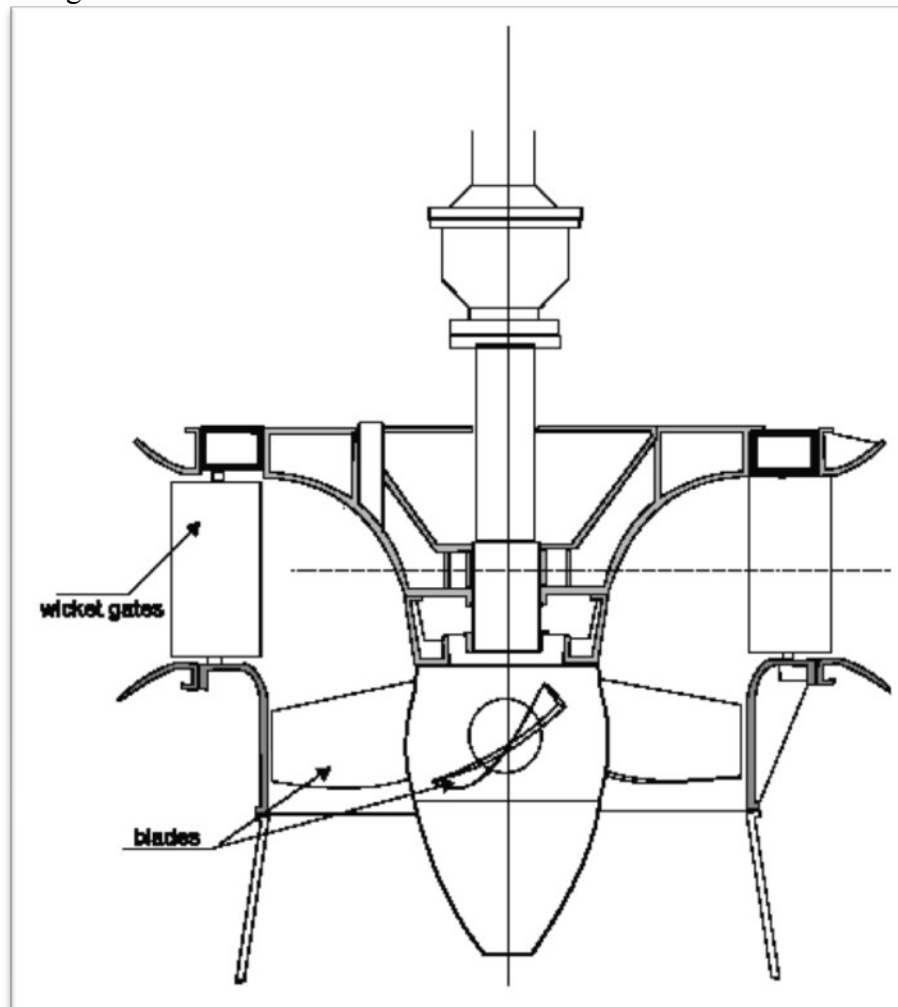


[Figure 2 - Kaplan Turbine](#)

### **Pumps working as turbine (PAT):**

Standard centrifugal pumps may be operated as turbines by directing flow through them from pump outlet to inlet. Since they have no flow regulation they can operate only under relatively constant head and discharge.

### **1.3.2 Impulse Principle:**

The water pressure is converted into kinetic energy before entering the runner. The kinetic energy is in the form of a high-speed jet that strikes the buckets, mounted on the periphery of the runner. Turbines that operate in this way are called impulse turbines. As the water after striking the buckets falls into the tail water with little remaining energy, the casing can be light and serves the purpose of preventing splashing.

### **Pelton turbines:**

Pelton turbines are impulse turbines where one or more jets impinge on a wheel carrying on its periphery a large number of buckets. Each jet issues through a nozzle with a needle (or spear) valve to control the flow. They are only used for relatively high heads. The axes of the nozzles are in the plane of the runner. To stop the turbine e.g. when the turbine approaches the runaway speed due to load rejection- the jet may be deflected by a plate so that it does not impinge on the buckets. In this way the needle valve can be closed very slowly, so that overpressure surge in the pipeline is kept to an acceptable minimum. Any kinetic energy leaving the runner is lost and so the buckets are designed to keep exit velocities to a minimum. The turbine casing only needs to protect the surroundings against water splashing and therefore can be very light.

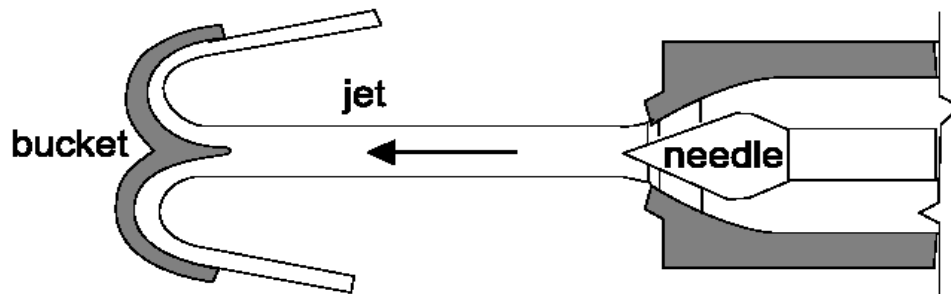


[Figure 3 - Pelton Turbine](#)

**Turgo turbines:**

The Turgo turbine can operate under a head in the range of 30-300 m. Like the Pelton it is an impulse turbine, but its buckets are shaped differently and the jet of water strikes the plane of its runner at an angle of  $20^\circ$ . Water enters the runner through one side of the runner disk and emerges from the other (Fig 6.6). (Compare this scheme with the one in Fig.6.5 corresponding to a Pelton turbine). Whereas the volume of water a Pelton turbine can admit is limited because the water leaving each bucket interferes with the adjacent ones, the Turgo runner does not present this problem. The resulting higher runner speed of the Turgo makes direct coupling of turbine and generator more likely, improving its overall efficiency and decreasing maintenance cost.

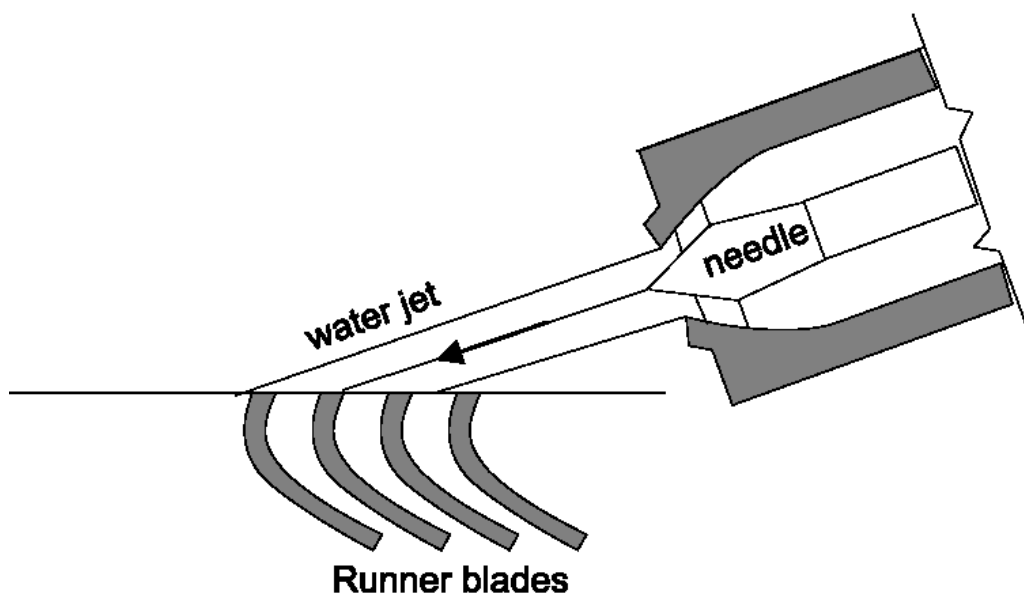


[Figure 4 - Turgo Turbine](#)

**Cross-flow turbines:**

This impulse turbine, also known as Banki-Michell in remembrance of its inventors and Ossberger after a company which has been making it for more than 50 years, is used for a wide range of heads overlapping those of Kaplan, Francis and Pelton. It can operate with discharges between 20 litres/sec and 10 m<sup>3</sup>/sec and heads between 1 and 200 m. Water (figure 6.7) enters the turbine, directed by one or more guide-vanes located in a transition piece upstream of the runner, and through the first stage of the runner which runs full with a small degree of reaction. Flow leaving the first stage attempt to crosses the open centre of the turbine. As the flow enters the second stage, a compromise direction is achieved which causes significant shock losses. The runner is built from two or more parallel disks connected near their rims by a series of curved blades). Their efficiency is lower than conventional turbines, but remains at practically the same level for a wide range of flows and heads (typically about 80%).



## Chapter 2

### LITERATURE REVIEW

The cross-flow turbine was invented about a century ago. Since the advent of cross flow turbines much advancement has been made in its design through experimental studies and research. Some of the published work is presented. Khosrowpanah [4] conducted a study on the effect on the number of blades, runner diameter, and nozzle entry arc under flow/ head variations on the performance of cross flow turbines. Four runners of width 6 inches were tested. In these experiments water was admitted vertically through a nozzle 6 inches wide with nozzle entry arc of 58, 78 and 90°. The results of these experiments concluded that the unit discharge increases with an increase in nozzle entry arc and runner aspect ratio and a decrease in the number of blades. The maximum efficiency of the cross flow turbine increases with an increase in the nozzle entry arc from 58 to 90 and decreases slightly with a decrease in runner diameter at constant runner width. For a runner diameter of 12 inches, the optimum number of blades was 15.

Nakase et al. [5] conducted experiments to study the effect of nozzle shape on the performance of cross-flow turbines. The outer diameter of the runner was 315mm and the runner had 26 blades, with blade inlet and outlet angles of 30 and 90 degrees. By classifying the flow as going through two stages, Nakase et al. [5] concluded that there are two types of flow in the cross-flow turbine. One is the crossed flow, which flows through two stages, and the other is uncrossed flow, which flows only through the first stage. The crossed flow constitutes a major portion of the flow which gives rise to flow contraction causing the flow to accelerate from the first stage to the second. Finally, Nakase et al. [5] concluded that the suitable value of nozzle throat width ratio ( $S_o/R\lambda$ ) is near 0.26 but changes slightly with the nozzle entry arc.

Laboratory studies on the efficiency of cross flow turbines were conducted by Akerkar [6]. The experimental study involved evaluating the effect of factors such as angle of attack, nozzle entry arc and nozzle entry configuration on the turbine efficiency. Three runners were constructed with angles of attack 16, 20 and 24 degrees. The outer diameter, inner to outer diameter ratio and the number of blades for the runners were 12 inches, 0.68 and 20 respectively. 5 nozzles were constructed with a throat width ratio 0.41. Akerkar [6] concluded that the flow pattern inside the cross flow turbine runner is concave when viewed from the shaft center. The jet angle at the first stage exit is greater for the vertical position of the nozzle than either the slant or the horizontal positions, indicating that there would be

more cross flow. The horizontal position of the nozzle was also concluded to be the least efficient.

Fiuzat and Akerkar [7] reported that the flow pattern inside the cross flow turbine runner is concave when viewed from the shaft center. The jet angle at the first stage exit is greater for the vertical position of the nozzle than either the slant or the horizontal positions, indicating that there would be more cross flow. The horizontal position of the nozzle was also concluded to be the least efficient. They also determined that at maximum efficiency, cross flow is about 40% and the speed ratio is between 0.45 and 0.55. The first stage of cross flow turbine produced 55% of the total power at 90 degrees nozzle entry arc and 59% at 120 degrees nozzle entry arc. The maximum efficiency attained without the interior guide tube was 89% for 90 degrees and with an angle of attack of 24 degrees. They [7] also reported that efficiency increased with an increase in the angle of attack from 16 to 24, thus contradicting Banki's theory of cross flow turbines.

Chappell [8] indicated that cross flow turbines manufactured out of standard Plexiglas plastic pipes or sheets can substantially reduce the cost of materials, manufacturing, and repairs. For micro-hydro power plants (less than 100kW in capacity), Chappell claims that the savings on the capital costs are in the order of about 50% or \$700/kW.

Simpson [9] mentions the case of an existing dam with adequate flow rates, as the best site for installing a cross flow turbine. This is attributed to the fact that cross flow turbines, can handle a wide range of flow rates and head values and is simple in construction and capable of self-cleaning. Simpson concludes that these reasons make the cross flow turbine an excellent turbine for run-of-stream hydro power plants with head values of more than 5ft.

Olgun [10,11] in his reported works concluded that; Cross-flow turbines can be operated efficiently in a wider range of gate openings than most turbines, maximum efficiency practically occurs at a constant speed for all gate openings at constant head, the speeds for maximum efficiency change with increasing the head at constant gate openings and the runner with diameter ratio 0.67 is more efficient than the runners with diameter ratios of 0.54, 0.58 and 0.75.

Durgin and Fay [12] constructed a cross-flow turbine in a configuration to allow extraction of the inter-stage cross flow and observation of the runner's internal flow patterns. The maximum efficiency attained was 61%. It was also determined that the second stage contributes approximately 17% of the total power. It was reported that a significant amount of entrained flow was carried by the runner, and did not cross to the second stage. An analysis was developed which incorporated the effects of entrained flow. This analysis was matched to the measured efficiency data. The efficiency predicted with the modified theory came out to be closer to the observed efficiency. The existing theory predicted a maximum

efficiency of 87% while the modified theory predicted an efficiency of 66% indicating that entrained flow must be accounted for in predictive techniques.

The experimental study of Aziz and Desai [13] reveals that in only 2 out of 18 cases, an increase in the diameter ratio produced an increase in the predicted maximum efficiency under automatic dynamometer speed control. They also concluded that somewhere in the vicinity of the diameter ratio of 0.68 the cross-flow is maximum and results in maximum efficiency due to second stage contribution. They also studied the effect of angle of attack on the turbine efficiency and concluded that the angle of attack should be around 24 degrees, an increase in the angle of attack from 24 to 32 degrees resulted in an increase in the predicted efficiency in only 2 out of 18 cases.

Thapar and Albertson [14] found that cross flow turbines are free from cavitations but are susceptible to wear when excessive silt and sand particles are present in the water. They also state that general maintenance is less complex than for other types of turbines as the runners are self cleaning.

## Chapter 3

# TURBINE DESIGN PARAMETERS

### 3.1 Site Data

According to the head, schemes can be classified in three categories:

- . High head:               100-m and above
- . Medium head:           30 - 100 m
- . Low head:                2 - 30 m

The site under consideration in the present work for installing a turbine is located in hyber Pakhtunkhwa with a head of 13.6m and can thus be categorized as a low head site. The volumetric flow rate available is 0.206m<sup>3</sup>/s.

### 3.2 Theoretical Power Output

The theoretical power output is an assumption of the energy potential of the site with alue of the micro-hydro scheme. It can be calculated using the site head and volumetric flow rate. Following formula is true for the calculation of theoretical power output:

$$P_t = \gamma \eta H Q$$

With an assumption of 80% efficiency, the theoretical power output comes out to be:

$$P_t = 21.94 \text{ kW}$$

### 3.3 Runner Outer Diameter

The following steps are involved in the calculation of the runner outer diameter:

- Selection of Generator rpm (Usually taken as 1500)
- Selection of Speed Ratio (6:1 in our case)
- Calculation of Runner rpm

The runner rpm is calculated using the generator rpm and the speed ratio, in our case the runner rpm is:

$$\text{Runner rpm} = 1500/6$$

$$\omega = 250$$

- Calculation of Water Jet Velocity:

The runner tangential velocity is calculated using the head of the site; the coefficient C accounts for the roughness in the water bed. Following is the formula used:

$$V_1 = C \sqrt{2gH}$$

With H=13.6m, g = 9.8m/s<sup>2</sup>, C=0.98, runner tangential velocity comes out to be:

$$V_1 = 16.06\text{m/s}$$

- Calculation of Runner Tangential Velocity:

First, the efficiency of the turbine is calculated as follows:

$$HP_{\text{out}} = \frac{\gamma Q u_1 \times V_1 \cos \alpha_1 \times \left(1 + \frac{\psi \cos \beta_2}{\cos \beta_1}\right)}{g}$$

$$HP_{\text{in}} = \frac{\gamma Q V_1^2}{C^2 2g}$$

$$\eta = \frac{HP_{\text{out}}}{HP_{\text{in}}}$$

This gives the following equation for efficiency:

$$\eta = \frac{2C^2 u_1 \left(1 + \frac{\psi \cos \beta_2}{\cos \beta_1}\right) \left(\cos \alpha_1 - \frac{u_1}{V_1}\right)}{V_1}$$

In the above eq. putting  $\beta_1 = \beta_2$ , Differentiating with respect to  $u_1/V_1$  and then equating to 0, gives the ratio  $u_1/V_1$  for maximum efficiency, which gives:

$$u_1 = 0.5V_1 \cos \alpha_1$$

Where, Angle of Attack  $\alpha_1 = 22^\circ$

Therefore, the runner tangential velocity comes out to be:

$$u_1 = 7.44\text{m/s}$$

- Calculation of Runner Outer Diameter:

The following formula relates the runner rpm and runner tangential velocity:

$$u_1 = r\omega$$

The turbine outer radius comes out to be:

$$r = 27\text{cm}$$

Therefore, the turbine outer diameter is:

$$D_1 = 54\text{cm}$$

### 3.4 Length of the Turbine Runner

A standard procedure in determining the length of the cross-flow turbine is as followed in Banki technical papers, which involves the calculation of the product of the turbine diameter and breadth. With the turbine outer diameter already calculated, this product can then be used to calculate the length of the runner:

The mathematical procedure is as follows:

$$L = \frac{144QN}{862 (0.98) (0.087) (\sqrt{2g})H}$$

$$\text{But, } N = \frac{2\sqrt{H}}{D_1}$$

Therefore,

$$LD_1 = \frac{210Q}{\sqrt{H}}$$

For our case, the calculation returns a turbine length of 35.5cm.

### 3.5 Runner Inner Diameter

The suggested inner to outer diameter ratio for a cross-flow hydraulic turbine is 0.7 (Aziz and Desai, 1991). Therefore:

$$\begin{aligned}\text{Runner Inner Diameter} &= (0.7)(54) \\ &= 37.8\text{cm}\end{aligned}$$

$$\begin{aligned}\text{Radial Rim Width} &= (54-37.8)/2 \\ &= 8.1 \text{ cm}\end{aligned}$$

### 3.6 Thickness of Water Jet

$$\begin{aligned}S_o &= 0.2D_1 \\ &= 0.2(54) \\ &= 10.8\text{cm}\end{aligned}$$

### 3.7 Spacing of Blades

$$\begin{aligned}S_1 &= kD_1 \\ &= (0.087)(54) \\ &= 4.7 \text{ cm}\end{aligned}$$

$$\begin{aligned}\text{Blade Spacing} = t &= S_1/\sin\beta_1 \\ &= 4.7/\sin 30^\circ \\ &= 9.4\text{cm}\end{aligned}$$

### 3.8 Number of Blades

Although the optimal number of blades can only be determined experimentally, following is the mathematical procedure presented in Banki technical paper:

$$n = \frac{\pi D_1}{t},$$

which gives number of blades to be 18. (The number of blades suggested by Aziz and inum efficiency is 24)

### 3.9 Radius of Blade Curvature

$$\begin{aligned} \rho &= 0.326r_1 \\ &= 0.326D_1/2 \\ &= 8.8\text{cm} \end{aligned}$$

### 3.10 Distance of Jet From Center of Shaft & Inner Periphery

#### 3.10.1 Distance of jet from centre of shaft:

$$\begin{aligned} y_1 &= (0.1986 - 0.945k)D_1 \\ &= \end{aligned}$$

#### 3.10.2 Distance of jet from inner periphery of the runner:

$$\begin{aligned} y_2 &= (0.1314 - 0.945k)D_1 \\ &= \end{aligned}$$

### 3.11 Angle of Attack

$$\eta = \frac{2C^2 u_1 \left(1 + \frac{\psi \cos \beta_2}{\cos \beta_1}\right) \left(\cos \alpha_1 - \frac{u_1}{V_1}\right)}{V_1}$$

The above equation for turbine efficiency implies that  $\alpha_1$  should be decreased in order to increase efficiency. The angle of attack may be decreased to  $22^\circ$  with convenience of construction therefore an angle of attack of  $22^\circ$  is chosen.

### 3.12 Angle between relative velocity of entering water jet and outer runner periphery ( $\beta_1$ ):

Since,  $u_1 = 0.5(V_1 \cos \alpha_1)$

From the velocity triangle (Fig. ?):

$$\tan \beta_1 = 2 \tan \alpha_1$$

putting  $\alpha_1 = 16^\circ$  gives  $\beta_1 = 30^\circ$ .



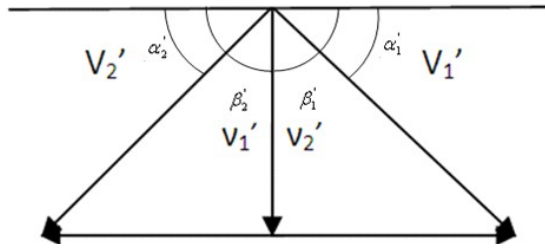


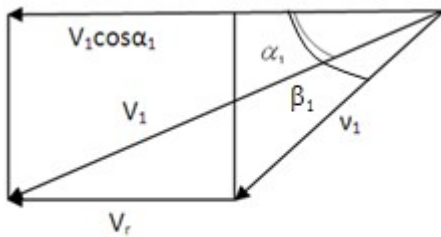
Figure 5 - Angle between relative velocity of entering water jet and outer runner periphery

### 3.13 First Stage Blade Exit Angle ( $\beta_2'$ )

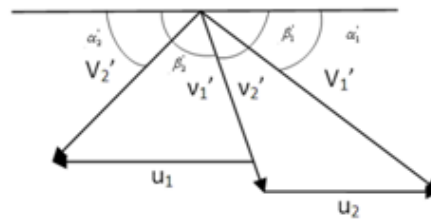
For a perfect radial flow  $\beta_2'$  should be equal to  $90^\circ$ . On account of the difference between the height of first stage exit and the second stage inlet the two velocities might differ i.e.,

$$V_1' = \sqrt{2gh_2 + V_2'^2}$$

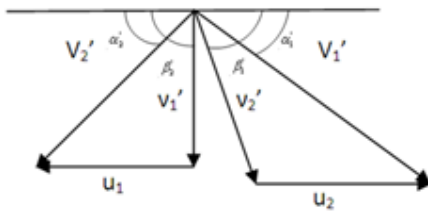
It is recommended that to increase the blade exit angle above  $90^\circ$  in order to prevent shock losses. Shock losses arise when the relative velocities of the first stage exit and second stage entrance are not concurrent. This concept is elaborated in Fig ?



a)  $V_2' = V_1'$



b)  $V_1' > V_2'$ ;  $v_1'$  and  $v_2'$  are non concurrent ( $\beta_2' = 90^\circ$ )



c)  $V_2' > V_1'$ ;  $v_1'$  and  $v_2'$  are concurrent ( $\beta_2' > 90^\circ$ )

Figure 6 – First Stage Blade Exit Angles

### **3.14 Runner Material**

Carbon Steel Castings are commonly used for turbine runners. ASTM A216 castings are of slightly higher strength than the more commonly used ASTM A27 material. ASTM A216 material is therefore used where increased mechanical strength is required. Keeping in view the unusually high flow-rate at the site under consideration, ASTM A216 is selected as the material for runner construction. Besides strength, it also provides relatively better resistance against corrosion and sand erosion.

## Chapter 4

### PERIPHERIAL EQUIPMENTS

#### 4.1 Penstock Design:

A penstock is a pipe that diverts the water from the main stream and carries it to the powerhouse where the turbine is located.

The main characteristics considered in selection of material are :-

- Young's Modulus of Elasticity
- Coefficient of linear expansion
- Ultimate Tensile strength
- Hazen Williams coefficient

Following are the materials considered :-

**Table 1 - Material Properties for Penstock Design**

Materials	Young's Modulus of Elasticity	Coefficient of linear expansion	Ultimate Tensile Strength	Hazen Williams coefficient (n)
Welded Steel	206	12	400	0.012
Cast Iron	78.5	10	140	0.014
Ductile Iron	16.7	11	340	0.015

The preference matrix analysis is then performed to select the most appropriate material, the material with the highest weighted score is selected. The results are tabulated in the tables below.

**Table 2 - Weighted Index, Welded Steel**

Criterion	Weight	Score	Weight x Score
Young's Modulus of Elasticity	15	1	15
Coefficient of linear expansion	15	0.833	12.5
Ultimate Tensile strength	40	1	40
Hazen Williams coefficient	30	0.75	22.5
Weighted Score			89.9

**Table 3- Weighted Index, Cast Iron**

Criterion	Weight	Score	Weight x Score
Young's Modulus of Elasticity	15	0.381	5.7
Coefficient of linear expansion	15	1	15
Ultimate Tensile strength	40	0.35	14
Hazen Williams coefficient	30	0.64	19.2
Weighted Score			53.9

**Table 4 - Weighted Index, Ductile Iron**

Criterion	Weight	Score	Weight x Score
Young's Modulus of Elasticity	15	0.081	1.22
Coefficient of linear expansion	15	0.91	13.65
Ultimate Tensile strength	40	0.85	34
Hazen Williams coefficient	30	0.6	18
Weighted Score			66.87

Based on these calculations, the welded steel has the highest weighted score and is therefore selected as the material for the penstock construction.

The Manning Equation can be used for the calculation of penstock diameter:

$$h_f/L = 10.3n^2Q^2/D_1^{5.333}$$

If pipe losses (due to friction and turbulence) are assumed to be 4% of the net head, then the equation comes out to be:

$$D = 2.69(n^2Q^2L/H)^{0.1875}$$

Taking length,  $L = 19.5\text{m}$

$$D = 2.69(0.012^2 * 0.208^2 * 19.5 / 13.63)^{0.1875}$$

$$D = 30.4\text{cm}$$

## 4.2 Power Transmission

There are two possible solutions for power transmission from the turbine shaft to the generator shaft, they are: Gears, Belts & Pulleys.

Gears are usually avoided in micro-hydro schemes due to their high cost and high maintenance. Belts and pulley mechanism, if properly designed, can well serve the purpose with efficiencies of about 98%.

- Types of Belts: Flat Belts, Vee-Belts (Wedge Belts is a type of vee belt that is usually used for micro-hydro applications)
- Types of Wedge Belts : SPZ, SPA, SPB, SPC (on basis of cross-sectional area)
- Calculate number of belts, belt length and belt tension:
  - Speed Ratio
  - Design Power = Power to be transmitted X Factors
  - Selecting Minimum Pulley Diameter
  - Find larger pulley diameter
  - Calculate approximate center distance
  - Obtain Rated Power/Belt
  - Calculate the number of belts
  - Calculate Belt Length
  - Calculate Belt tension

Following are the mathematical calculations involved:

$$\text{Speed Ratio} = 6:1$$

$$\text{Design Power} = (22)(1.18)(1.2) \text{ [Where, Service Factor} = 1.18 \text{ \& Duty Factor} = 1.2]$$

$$= 31.152\text{kW}$$

Belt type selected: SPB Wedge Belt [From Fenner Belt Selection Envelopes]

Min. Pulley Diameter: 140mm [From Fenner Wedge Belt Catalogue]

Rated Power/Belt = 7.09kW/Belt [From Fenner Wedge Belt Catalogue]

Number of Belts = Design Power/Rated Power per Belt

$$N = 5$$

Larger Pulley Diameter:  $6(140) = 840\text{mm}$

Approx. Center Distance =  $(D+d)/2$

$$C = 980\text{mm}$$

$$\text{Belt Length} = 2C + \pi(D+d)/2 + (D-d)^2/4C$$

$$= 3.62\text{m}$$

Belt Tension =  $32PN$

$$= 10.4\text{kN}$$

Where, P is the force required to deflect the belt 16mm of the entire belt span. The formula and value of P is taken from the Fenner Wedge Belt Catalogue

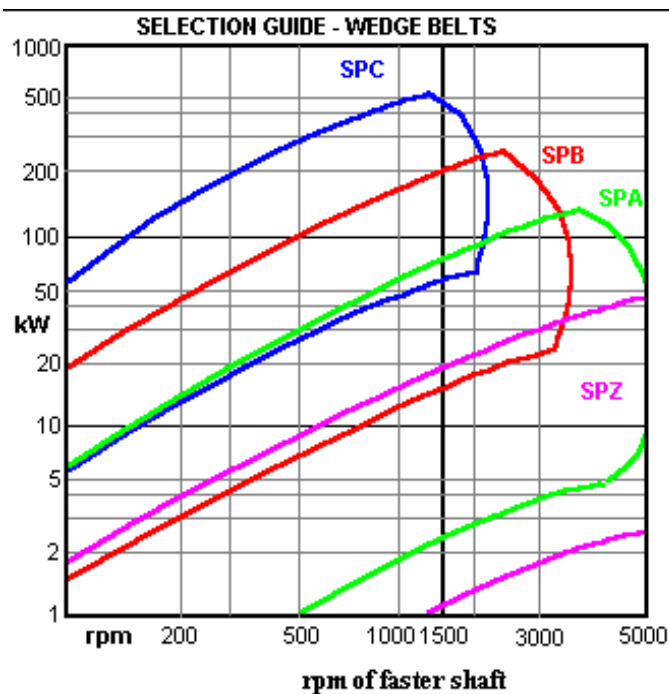


Figure 7 - Belt Selection Envelopes (Fenner Wedge Belt Catalogue)

### 4.3 Shaft Design

The shaft design has been based on the maximum bending moment criterion and returns a conservative result. Following is the procedure followed (Adam Harvey, Micro-Hydro Design Manual, 1999):

- Calculation of Belt Tension
- Calculation of Bearing Loads
- Calculation of Maximum Bending Moment
- Calculation of shaft diameter using the following formula:

$$d = [5.1/t_p \{(C_m M)^2 + (C_t F)^2\}^{0.5}]^{0.33}$$

Belt Tension = 10.4kW

Bearing Loads:

$$R_a = 10.156\text{kN}$$

$$R_b = 6.616\text{kN}$$

Maximum Bending Moment:

$$M_r = 0$$

$$M_a = 354\text{Nm}$$

$$M_{\text{belt}} = 473\text{Nm (Maximum)}$$

$$M_b = 0$$

Shaft Diameter = 69mm

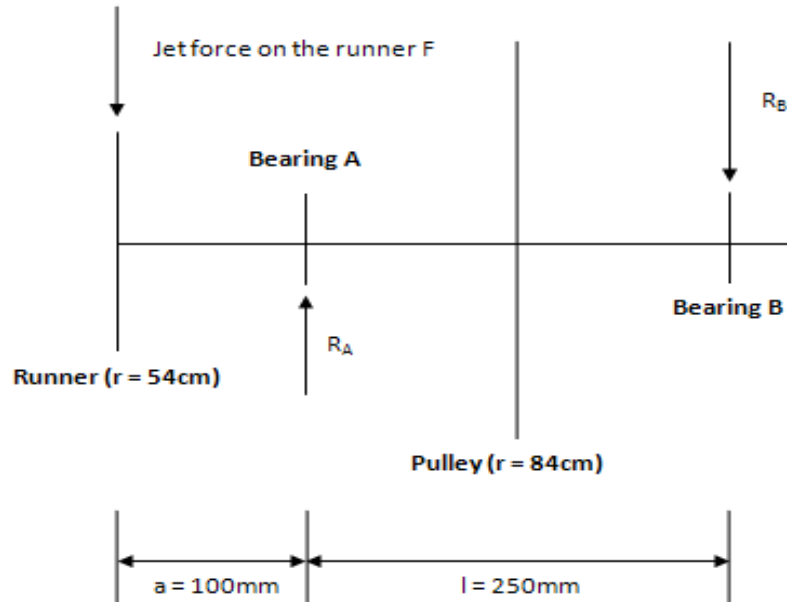


Figure 8 - Runner Shaft Arrangement

#### 4.3.1 Shaft Deflection

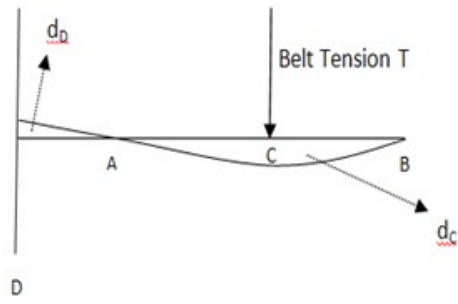
Shaft Design is considered to be acceptable if deflection in the shaft doesn't exceed  $(0.0005 * \text{Distance between the bearings})$ .

Following are the formulae used for shaft deflection (Allen R. Inversin, Micro-Hydro Power Sourcebook, 1995):

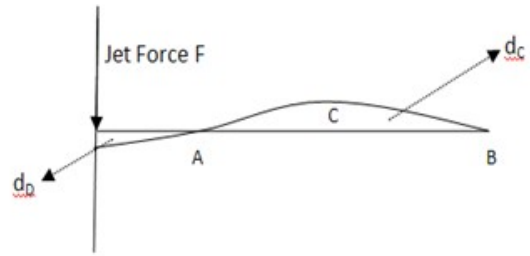
- $d_{CT} = -Tl^3/48EI$
- $d_{Dt} = +Tal^2/16EI$
- $d_{CF} = +Fal^2/16EI$
- $d_{DF} = -Fal^2(1+a)/3EI$

The total shaft deflection comes out to be  $0.012\text{mm}$





Shaft Deflection in presence of Belt Tension Only



Shaft Deflections in presence of Jet Force Only

Figure 9 - Shaft Deflection

## **Chapter 5**

# **CAD MODELS FOR MANUFACTURING**

After the design parameters of the turbine were calculated, the CAD models were generated using Pro-e CAD software. A local manufacturer by the name of Gulzaar Khan of CHIRACH ENGINEERING WORKS was then trained to manufacture the designed turbine. A template of side plate of the turbine runner was also manufactured using NC Wire-Cut machine available in the GIK institute's Industrial CNC laboratory.

The important components of the Cross-Flow Turbine are discussed under in reference to the CAD;

### **5.1 Side Plates:**

The side plate is the most important component for accurate placement of the runner blades. Following are the steps that ensure the accurate modeling and thus manufacturing of the side plates.

Step1.

Step2.

Step3.

Step4.

Step5.

Step6.

Step7.

Step8.

**CAD model of Side Plate:**

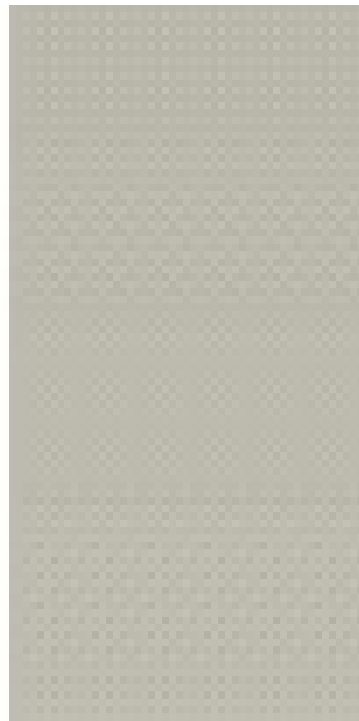


**Figure 10 - Side Disk CAD Model**

**5.2 Runner Blade:**

Next, the runner blade was modeled with dimensions shown in the figure below.

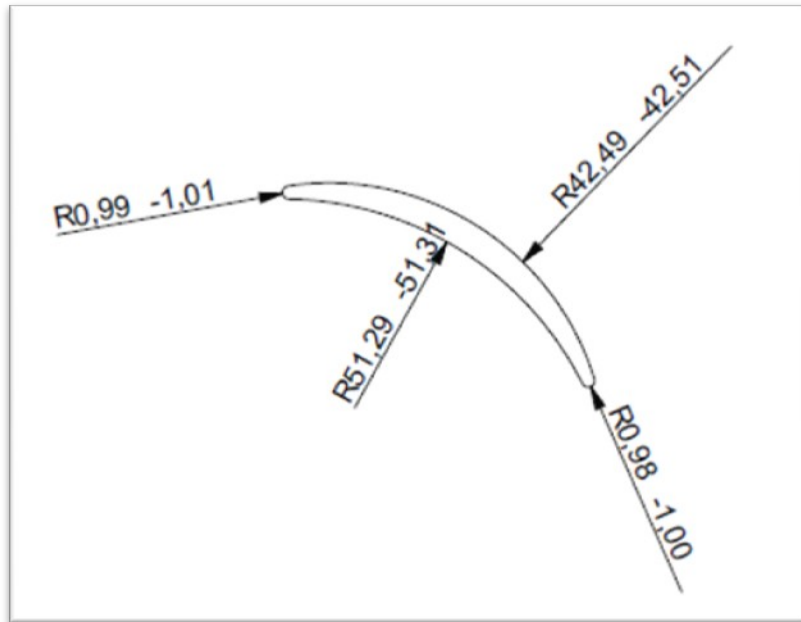


[Figure 11 - Runner Blade Dimensioning](#)

### 5.3 Runner Shaft:

Maximum Diameter: 70mm

Minimum Diameter: 40mm

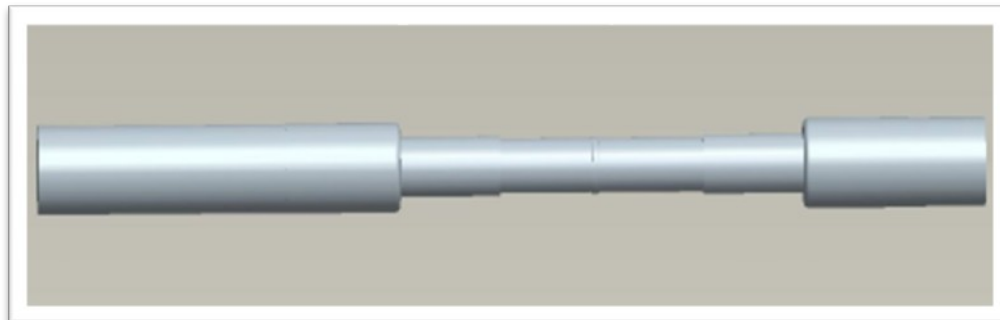


[Figure 12 - Runner Shaft](#)

### Complete Runner Assembly:

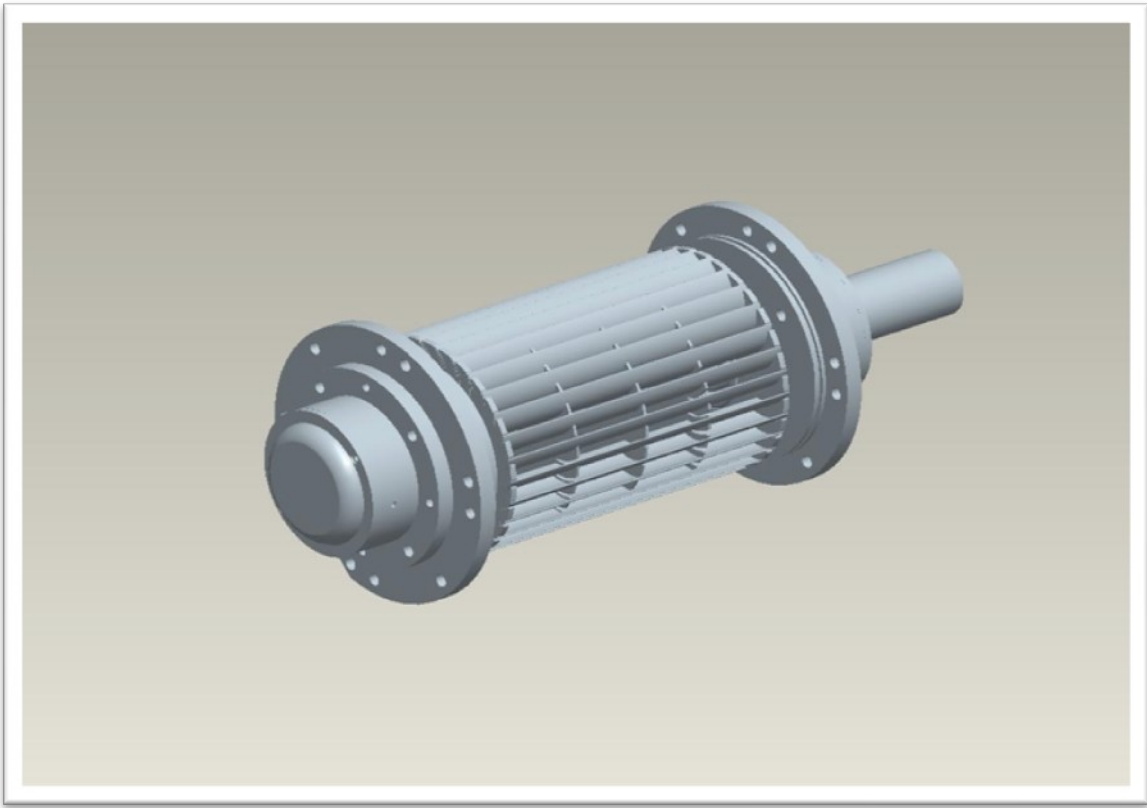


Figure 13 - Complete Runner Assembly

**Complete Turbine Assembly:**



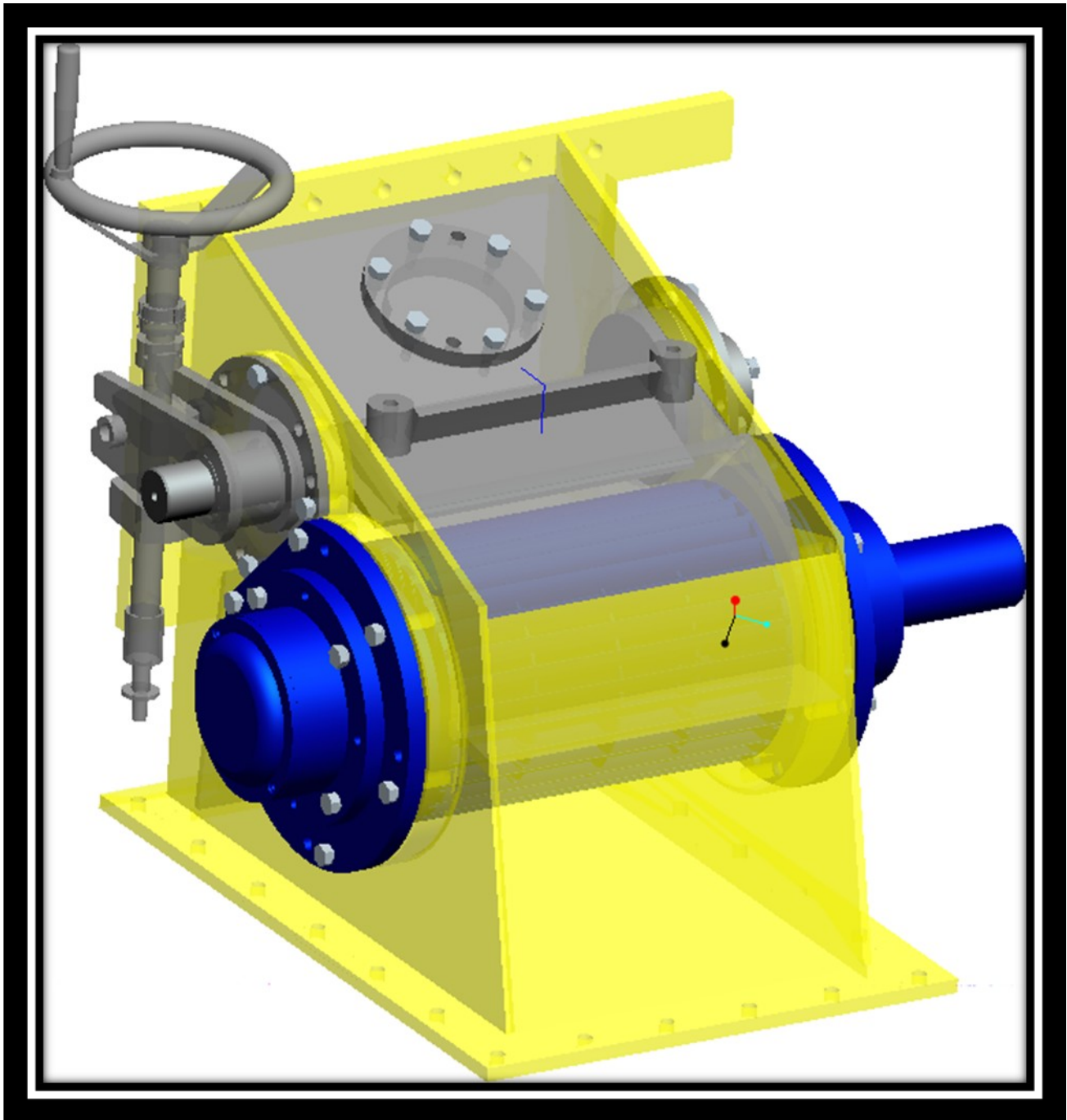


Figure 14 - Complete Turbine Assembly

**Chapter 6**  
**SOFTWARE**

The current manufacturers in Pakistan are not outfitted with any engineering background. The existing design is largely based on experience rather than any expert technical knowledge.

By means of all the extensive literature research that we've conducted throughout the course of our project, we have been able to identify some optimum design parameters that help amplify the efficiency of CFHTs.

An Interactive software has, thus, been developed that incorporates these optimal design values and helps, even a layman, calculate and identify the best design parameters for the site under consideration.

The following methodology has been adapted to develop this software:

- Determining the Head Loss and thus, the Net Head
- Calculation of the Outer and Inner Diameters
- Calculation of the Width of the Runner
- Calculation of the Blade Inlet Angle
- Calculation of the Spacing of Blades and thus, the Number of Blades on the runner
- Calculation of the Nozzle Width
- Calculation of the Diameter of the Penstock using its input length
- Calculation of the Expected Power Output

The following figures illustrate a sample case:

The screenshot shows a software window titled "Micro Hydro Software Version 1.1". The main heading is "MICRO HYDRO SOFTWARE v1.1" with a "Help" button to the right. Below this is the sub-heading "DESIGN A CROSSFLOW TURBINE". The interface contains a list of input parameters, each with a text box for the value and a "Calculate" button at the bottom left. A note at the bottom right states "\*Enter all values in SI units".

Parameter	Value	Notes
Gross Head	13.7	
Channel Area	0.929	
Flow Rate	0.206	
Speed Ratio	6	3-6 (Recommended)
Expected Efficiency	0.8	
Length of Penstock	20	
Generator RPM	1550	1550 RPM (Recommended)
Angle of Attack	22 Degrees	
Blade Exit Angle	55 Degrees	
Nozzle Entry Arc	90 Degrees	
Diameter Ratio	0.7	
Friction Factor	0.15	

Figure 15 - Input Form



Figure 16 - Output (SI Units)

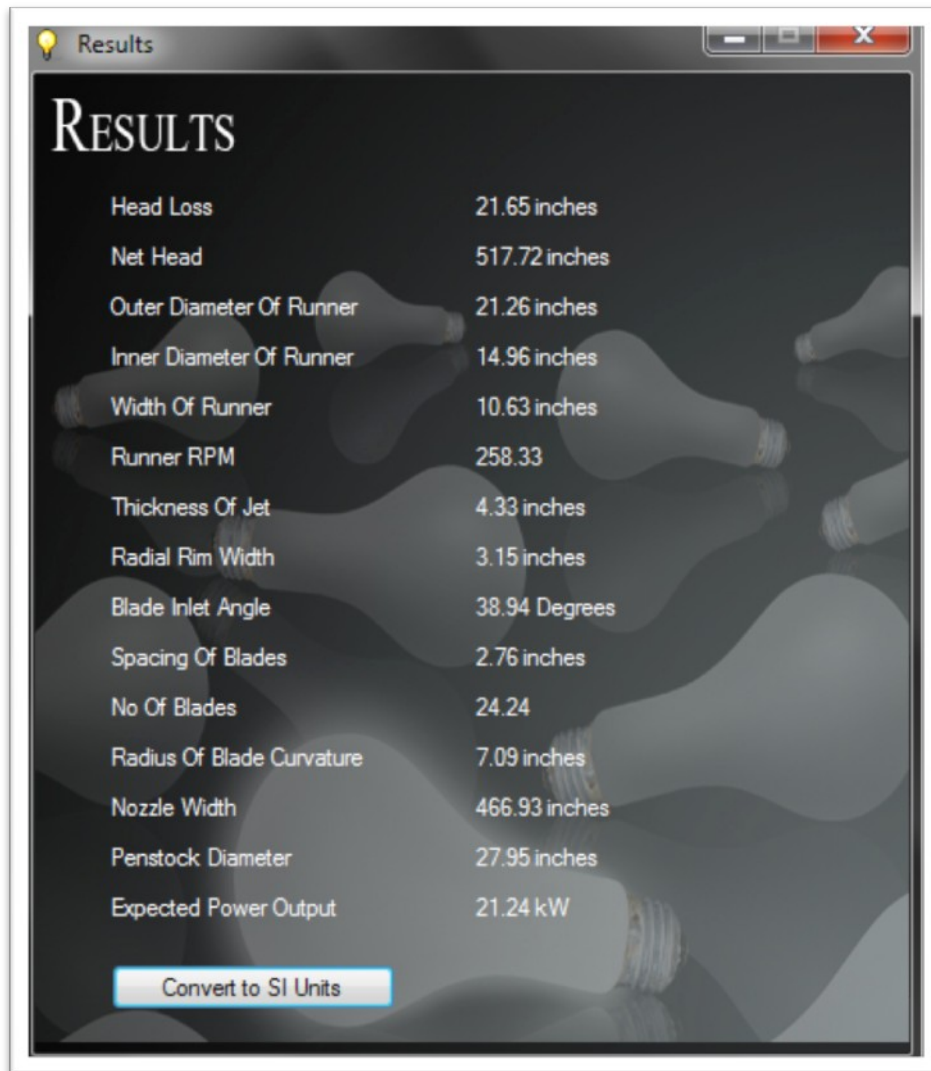


Figure 17 - Output (English Units)

A help file has also been created that will help the user understand the terms used in the software.

(The entire content of the help file can be found in Appendix B2)

## **Chapter 7**

### **CONCLUSION**

By extensive literature research and consultation with the field experts, we were able to design and manufacture a more efficient Cross Flow Turbine than available in the local market. Further work is needed to standardize this turbine in Pakistan and train the local manufacturers to adopt this design.

## REFERENCES

- [1] J.A. Chattha, M.S. Khan, "Experimental study to test an axial flow pump as a turbine and development of performance characteristics for micro-hydro power plant" Proceedings of the ASME Power 07 Conference July 17-19, 2007, San Antonio, Texas, USA
- [2] J.A. Chattha, M.S. Khan and A. Haque, " Micro-hydro power systems: Current status and future research in Pakistan " Proceedings of the ASME Power 09 Conference July 21-23, 2009, Albuquerque, New Mexico, USA
- [3] OSSBERGER cross-flow turbine. <http://www.ossberger.de/cms/en/hydro/the-ossberger-turbine/#c152>
- [4] Khosrowpahan, S., "Experimental Study of the Crossflow Turbine", Ph.D. Dissertation, Colorado State University, Fort Collins, CO, 1984.
- [5] Nakase, Y., Fukutomi, J., Wantanabe, T., Suessugu, T., and Kubota, T., "A study of Crossflow Turbine", Small Hydro Power Fluid Machinery, p. 13-18, 1982.
- [6] Akerkar, B. P., "A Study of the Performance of the Crossflow Turbine", M.S. thesis, Clemson University, Clemson, SC, 1989.
- [7] Fiuzat, A.A., and Akerkar B.P., "The Use of Interior Guide Tube in Crossflow Turbines", International Conference on Hydropower; Waterpower 1989 . p. 1111-1119
- [8] Chappell, J. R., "Recent DOE-Sponsored Hydropower Engineering Research", Report No. ECG-M-02983, p6, 1983
- [9] Simpson, B. J., "Low Head, Micro-Hydro Demonstration Project, Coker Alabama, Final Report", Report No. DOE/R4 10233-TI, 1983
- [10] Hayati Olgun, "Effect of interior guide tubes in cross-flow turbine runner on turbine performance", International Journal of Energy Research, p 953-964, 2000 John Wiley & Sons
- [11] Hayati Olgun, "Investigation of the Performance of a Cross-Flow Turbine", International Journal of Energy Research, pp 953-964, 1998 John Wiley & Sons
- [12] Durgin W.W and Fay W.K, "Some Fluid Flow Characteristics of a Cross-Flow Type Hydraulic Turbine" Small Hydro Power Fluid Machinery, 1984, p77-83. The Winter Annual meeting of ASME, New Orleans, L.A, December 9-14, 1984
- [13] Nadim M. Aziz and V. R. Desai, "An Experimental Study of the Effect of Some Design Parameters in Cross-Flow Turbine Efficiency", Engineering Report, Department of Civil Engineering, Clemson University, 1991.
- [14] Thapar, O.D., and Albertson, M.L., "Ultra Low Head Small Hydro Power System Technology for Economic Development", Waterpower 1985
- [15] Mockmore C. A., and Merryfield, F., "The Banki water turbine." Engineering experimental station bulletin series No. 25, February 1949, p 22

# APPENDIX A

Technical Paper for Asme Power 2010 Conference, Chicago, IL, USA (July 13-15)

Proceedings of ASME 2010 Power Conference  
POWER2010-27184  
July 13-15, 2010, Chicago, Illinois, USA

## DESIGN OF A CROSS FLOW TURBINE FOR A MICRO-HYDRO POWER APPLICATION

Javed A. Chattha, Mohammad S. Khan, Syed T. Wasif, Osama A. Ghani, Mohammad O. Zia, Zohaib Hamid  
Faculty of Mechanical Engineering  
GIK Institute of Engineering Sciences & Technology  
Topi, NWFP, Pakistan

### ABSTRACT

The total installed capacity of the hydropower stations in Pakistan is about 7,000 MW which is about 20% of the total available hydro power potential. For possible micro-hydro stations, a potential of about 1300 MW exists at a number of low head and high flow rate sites. Work has been reported by Chattha et al. [1,2] related to installation of a micro-hydro power station at one of the typical sites. An axial flow pump-as-turbine (PaT) was installed to generate electrical power at the micro-hydro station. The site selected for this work is quite typical and efforts are now being made to utilize the maximum potential of the site conditions. The PaT only utilizes about half of the available flow of water and a spillway was constructed at this site to divert the excess amount of water. The diverted water flows back to the main stream after bypassing the PaT. Work is now being carried out to explore the installation of a turbine in the spillway to harness the energy potential of the diverted water stream. This work includes selection, design, fabrication and installation of a turbine in order to generate electrical power utilizing the energy of water diverted to the spillway. A 100 ft<sup>3</sup>/sec flow rate with about 11 ft head is available at the spillway side. Considering these site conditions and indigenous fabrication expertise, cross flow type turbine has been selected for installation. Cross flow turbines are being manufactured in Pakistan and are usually quite successful for micro-hydro systems. Based on the available site conditions, a cross flow turbine has been designed. The diameter and length of the turbine runner have been calculated. Furthermore, the number

of blades and radius of curvature have been determined along with other design parameters. The designed turbine is expected to produce about 50 kW of power. The complete design of the turbine, based on the available site conditions is presented in this paper.

### Nomenclature:

**a** - Radial Rim Width  
**C** - Coefficient accounting for nozzle roughness  
**D<sub>2</sub>** - Inner Diameter of the runner  
**d<sub>1</sub>** - Penstock Pipe diameter  
**H** - Head  
**h<sub>2</sub>** - vertical distance between 1<sup>st</sup> stage inlet and 2<sup>nd</sup> stage exit  
**HP<sub>out</sub>** - Output Horse Power  
**N** - Angular speed of the runner  
**n** - Number of blades  
**P<sub>t</sub>** - Theoretical Power Output  
**Q** - Flow Rate  
**S<sub>o</sub>** - Thickness of jet  
**s<sub>t</sub>** - Tangential blade spacing  
**t** - Blade spacing  
**u<sub>1</sub>** - Tangential velocity of runner outer periphery  
**u<sub>1</sub>'** - tangential velocity of runner inner periphery  
**V** - Absolute velocity of water along the channel  
**V<sub>1</sub>** - Absolute velocity of the entering water jet  
**V<sub>1</sub>'** - Absolute velocity of entering water jet (2<sup>nd</sup> stage)  
**V<sub>2</sub>'** - Absolute velocity of water from first stage exit  
**v<sub>1</sub>** - relative velocity of the entering water jet



$v_1'$  - relative velocity of the entering water jet (2<sup>nd</sup> stage)  
 $v_2'$  - relative velocity of the water from first stage exit  
 $y_1$  - Distance of jet from centre of the shaft  
 $y_2$  - Distance of jet from inner periphery of the runner

Greek symbols

$\alpha_1$  - angle of attack  
 $\alpha_2'$  - Angle between runner inner periphery and absolute velocity exiting water jet (1<sup>st</sup> stage)  
 $\beta_1'$  - angle between runner inner periphery and relative velocity of entering water jet (2<sup>nd</sup> stage)  
 $\beta_2'$  - angle between runner inner periphery and relative velocity of exiting water jet (1<sup>st</sup> stage)  
 $\alpha_1'$  - Angle between runner inner periphery and absolute velocity of entering water jet (2<sup>nd</sup> stage)  
 $\eta$  - Assumed System Efficiency  
 $\gamma$  - Specific weight of water  
 $\psi$  - Coefficient accounting for blade roughness  
 $\rho$  - Radius of blades curvature

## INTRODUCTION

Pakistan is endowed with a hydro potential of approximately 42,000 MW, most of which lies in the NWFP, Northern areas, Azad Jammu Kashmir and Punjab. The total installed capacity of the hydropower stations in the country is about 7,000 MW [2]. The potential sites consist of high, medium and low head conditions. The majority of low head sites are located in remote areas of Pakistan which are off grid and suitable for axial flow turbine conditions. An estimated power production of 1,300 MW can be produced by installing turbines on these micro-hydro sites [2]. The objective of the present study is to design a cross flow turbine which will be later fabricated and installed at a site where a PaT has already been installed and provision of installing another turbine exists.

Hydropower is considered as one of the most desirable sources of energy due to its environment-friendly nature and extensive potential available throughout the globe. Within the scope of hydropower, Micro-Hydro Power Plants have gained much attention in recent years. There is no consensus on the definition of a *micro-hydro* power plant, but generally 1MW is accepted as the upper limit for a power plant to be termed as *micro-hydro*.

Several solutions have been proposed and successfully implemented for micro-hydro schemes, which include radial flow turbines and axial flow or propeller type turbines. At present, the cross-flow hydraulic turbine is gaining popularity in small and ultra-low head establishments due to its remarkably simple structure and the ease of manufacturing that it provides.

The cross-flow turbine was invented about a century ago. The cross-flow hydraulic turbine is composed of two major parts, the runner and the nozzle. The

runner is a circular rotor with two sidewalls to which the blades are fixed along the periphery of the turbine. The cross-section of these blades is circular with a specific radius of curvature and the blades are aligned at an angle with the tangent to the outer periphery of the turbine. The nozzle directs the flow into the runner at a certain angle of attack. It has a rectangular cross-section with curved back wall.

The cross-flow turbine is a two stage hydraulic turbine. Typical components of a cross-flow turbine are shown in Figure 1[3]. The water jet leaving the nozzle strikes the blades at the first stage. The water exits the first stage and is 'crossed' to the second stage inlet after which it exits the runner completely. Some of the water is entrained between the turbine stages and does not contribute to the energy generation. This is termed as 'uncrossed' flow. One of the major design considerations in Cross-Flow Hydraulic Turbines is minimizing this undesirable uncrossed flow in order to achieve maximum efficiency.

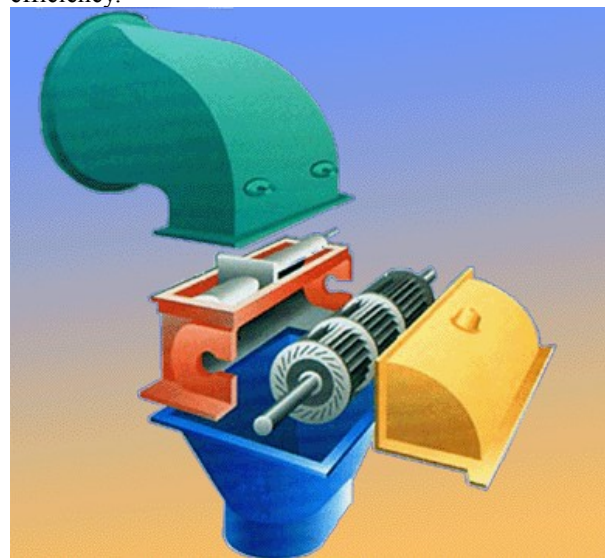


Fig. 1: Typical components of a cross-flow turbine [3]

The efficiency of the cross-flow hydraulic turbine is dependent on several design parameters. These include runner outer diameter, breadth of the runner, thickness of water jet, number of blades, spacing of blades in the runner, radius of blades curvature, angle of attack, the first stage blade exit angle and angle between relative velocity of entering water jet and turbine outer periphery. These design parameters have been analyzed in this paper and selections have been made based on quantitative methods and experimental studies already carried out by different researchers. There are several other important considerations for a micro-hydro power plant. One of the most important of which is the penstock design. It is imperative to minimize the head loss that occurs due to friction between the pipe surface and flowing fluid. Material

selection is also an important factor while designing a micro-hydro scheme. These factors have also been discussed in this paper.

Since the advent of cross flow turbines much advancement has been made in its design through experimental studies and research. Some of the published work is presented. Khosrowpanah [4] conducted a study on the effect on the number of blades, runner diameter, and nozzle entry arc under flow/ head variations on the performance of cross flow turbines. Four runners of width 6 inches were tested. In these experiments water was admitted vertically through a nozzle 6 inches wide with nozzle entry arc of 58, 78 and 90°. The results of these experiments concluded that the unit discharge increases with an increase in nozzle entry arc and runner aspect ratio and a decrease in the number of blades. The maximum efficiency of the cross flow turbine increases with an increase in the nozzle entry arc from 58 to 90 and decreases slightly with a decrease in runner diameter at constant runner width. For a runner diameter of 12 inches, the optimum number of blades was 15.

Nakase et al. [5] conducted experiments to study the effect of nozzle shape on the performance of cross-flow turbines. The outer diameter of the runner was 315mm and the runner had 26 blades, with blade inlet and outlet angles of 30 and 90 degrees. By classifying the flow as going through two stages, Nakase et al. [5] concluded that there are two types of flow in the cross-flow turbine. One is the crossed flow, which flows through two stages, and the other is uncrossed flow, which flows only through the first stage. The crossed flow constitutes a major portion of the flow which gives rise to flow contraction causing the flow to accelerate from the first stage to the second. Finally, Nakase et al. [5] concluded that the suitable value of nozzle throat width ratio ( $S_0/R\lambda$ ) is near 0.26 but changes slightly with the nozzle entry arc.

Laboratory studies on the efficiency of cross flow turbines were conducted by Akerkar [6]. The experimental study involved evaluating the effect of factors such as angle of attack, nozzle entry arc and nozzle entry configuration on the turbine efficiency. Three runners were constructed with angles of attack 16, 20 and 24 degrees. The outer diameter, inner to outer diameter ratio and the number of blades for the runners were 12 inches, 0.68 and 20 respectively. 5 nozzles were constructed with a throat width ratio 0.41. Akerkar [6] concluded that the flow pattern inside the cross flow turbine runner is concave when viewed from the shaft center. The jet angle at the first stage exit is greater for the vertical position of the nozzle than either the slant or the horizontal positions, indicating that there would be more cross flow. The horizontal position of the nozzle was also concluded to be the least efficient.

Fiuzat and Akerkar [7] reported that the flow pattern inside the cross flow turbine runner is concave when viewed from the shaft center. The jet angle at the first stage exit is greater for the vertical position of the nozzle than either the slant or the horizontal positions, indicating that there would be more cross flow. The horizontal position of the nozzle was also concluded to be the least efficient. They also determined that at maximum efficiency, cross flow is about 40% and the speed ratio is between 0.45 and 0.55. The first stage of cross flow turbine produced 55% of the total power at 90 degrees nozzle entry arc and 59% at 120 degrees nozzle entry arc. The maximum efficiency attained without the interior guide tube was 89% for 90 degrees and with an angle of attack of 24 degrees. They [7] also reported that efficiency increased with an increase in the angle of attack from 16 to 24, thus contradicting Banki's theory of cross flow turbines.

Chappell [8] indicated that cross flow turbines manufactured out of standard Plexiglas plastic pipes or sheets can substantially reduce the cost of materials, manufacturing, and repairs. For micro-hydro power plants (less than 100kW in capacity), Chappell claims that the savings on the capital costs are in the order of about 50% or \$700/kW.

Simpson [9] mentions the case of an existing dam with adequate flow rates, as the best site for installing a cross flow turbine. This is attributed to the fact that cross flow turbines, can handle a wide range of flow rates and head values and is simple in construction and capable of self-cleaning. Simpson concludes that these reasons make the cross flow turbine an excellent turbine for run-of-stream hydro power plants with head values of more than 5ft.

Olgun [10,11] in his reported works concluded that; Cross-flow turbines can be operated efficiently in a wider range of gate openings than most turbines, maximum efficiency practically occurs at a constant speed for all gate openings at constant head, the speeds for maximum efficiency change with increasing the head at constant gate openings and the runner with diameter ratio 0.67 is more efficient than the runners with diameter ratios of 0.54, 0.58 and 0.75.

Durgin and Fay [12] constructed a cross-flow turbine in a configuration to allow extraction of the inter-stage cross flow and observation of the runner's internal flow patterns. The maximum efficiency attained was 61%. It was also determined that the second stage contributes approximately 17% of the total power. It was reported that a significant amount of entrained flow was carried by the runner, and did not cross to the second stage. An analysis was developed which incorporated the effects of entrained flow. This analysis was matched to the measured efficiency data. The efficiency predicted with the modified theory came out to be closer to the observed efficiency. The existing theory predicted a maximum

efficiency of 87% while the modified theory predicted an efficiency of 66% indicating that entrained flow must be accounted for in predictive techniques.

The experimental study of Aziz and Desai [13] reveals that in only 2 out of 18 cases, an increase in the diameter ratio produced an increase in the predicted maximum efficiency under automatic dynamometer speed control. They also concluded that somewhere in the vicinity of the diameter ratio of 0.68 the cross-flow is maximum and results in maximum efficiency due to second stage contribution. They also studied the effect of angle of attack on the turbine efficiency and concluded that the angle of attack should be around 24 degrees, an increase in the angle of attack from 24 to 32 degrees resulted in an increase in the predicted efficiency in only 2 out of 18 cases.

Thapar and Albertson [14] found that cross flow turbines are free from cavitations but are susceptible to wear when excessive silt and sand particles are present in the water. They also state that general maintenance is less complex than for other types of turbines as the runners are self cleaning.

The objective of a hydro power scheme is to convert the potential energy of a mass of water, flowing in a stream with a certain fall (termed the 'head'), into electric energy at the lower end of the scheme, where the powerhouse is located. The power of the scheme is proportional to the flow and to the head.

According to the head, schemes can be classified in three categories:

- . High head: 100-m and above
- . Medium head: 30 - 100 m
- . Low head: 2 - 30 m

The site under consideration in the present work for installing a turbine has a head of 3.35m and can thus be categorized as a low head site. The volumetric flow rate available is 2.83m<sup>3</sup>/s. While designing a cross flow turbine the major considerations include the turbine runner design, shaft design, power transmission mechanism, bearing selection, material selection and electrical generator selection for a particular case. The turbine design procedure followed in this work is that of Banki translated in [15].

#### Theoretical Power Output:

Following equation is true for the calculation of theoretical power output:

$$P_t = \lambda \eta H Q$$

Assuming  $\eta=60\%$  gives a  $P_t$  of 55.8 kW. This implies that with a modest assumption of 60% system efficiency, the site under consideration has an approximate potential of 56 kW.

#### Turbine Selection:

The first step in the design of micro-hydro power plant is the selection of the appropriate turbine that complements the head and flow available at the site, available site potential as well as the locally available manufacturing facilities. The site under consideration falls under the Cross-Flow Turbine Convenience of manufacturing and economic factors is also to be considered in addition to the site parameters while selecting the turbine.

#### Runner Dimensions:

Outer Diameter of the Runner ( $D_1$ ):

A standard procedure in determining the diameter of the cross-flow turbine is as followed in Banki technical papers, which involves the calculation of the product of the turbine diameter and breadth. Different combinations of Diameter ( $D_1$ ) and breadth ( $l$ ) are then considered and finally the most feasible combination is then selected.

The mathematical procedure is as follows:

$$L = \frac{144QN}{862 (0.98)(0.087)(\sqrt{2g})H}$$

$$\text{But, } N = \frac{2\sqrt{H}}{D_1}$$

Therefore,

$$LD_1 = \frac{210Q}{\sqrt{H}}$$

For our case, we get  $LD_1 = 4 \text{ m}^2$ . The results for various combinations of runner breadth and outer diameter have been tabulated (Table 1). Clearly, none of the alternatives is feasible. The anomaly arises particularly due to relatively high flow rate observed at the site.

Table 1: Various combinations of runner breadth and diameter

$LD_1 \text{ (m}^2\text{)}$	$L \text{ (m)}$	$D_1 \text{ (m)}$
4	2	2
4	2.5	1.6
4	3	1.33
4	3.5	1.14

Water velocity:

$$V_1 = C \sqrt{2gH}, \text{ i.e., } = 8 \text{ m/s}$$

#### Runner Tangential Velocity:

First, the efficiency of the turbine is calculated as follows:

$$HP_{out} = \frac{\rho Q u_1 \times V_1 \cos \alpha_1 \times (1 + \frac{\psi \cos \beta_2}{\cos \beta_1})}{g}$$

$$HP_{in} = \frac{\rho Q V_1^2}{C^2 2g}$$

$$\eta = \frac{HP_{out}}{HP_{in}}$$

This gives the following equation for efficiency:

$$\eta = \frac{2C^2 u_1 (1 + \frac{\psi \cos \beta_2}{\cos \beta_1}) (\cos \alpha_1 - \frac{u_1}{V_1})}{V_1}$$

In the above eq. putting  $\beta_1 = \beta_2$ , Differentiating with respect to  $u_1/V_1$  and then equating to 0, gives the ratio  $u_1/V_1$  for maximum efficiency, which gives:

$$u_1 = 0.5 V_1 \cos \alpha_1$$

This clearly indicates that  $\alpha_1$  should be kept as small as possible for maximum efficiency. Experimental research has shown that arc angles of  $16^\circ$  can be obtained without much inconvenience of manufacturing. Therefore, for  $\alpha_1 = 16^\circ$  and  $V_1 = 8\text{m/s}$ ,  $u_1$  comes out to be  $3.84\text{ m/s}$ .

### Runner angular velocity:

The calculation of runner angular velocity is based on the following assumptions:

Generator rpm: 1550

Velocity ratio: 6:1

Therefore runner rpm =  $1550/6 = 258\text{ rpm}$

### Runner Outer Diameter (D<sub>1</sub>):

Since  $u_1 = r\omega$ , therefore  $r = \frac{u_1}{\omega}$ , i.e.,  $r = 0.1422\text{m}$

Therefore  $D_1$  comes out to be  $28.5\text{cm}$

### Breadth of the runner(L):

For a  $1.22\text{m}$  wide channel, runner breadth is taken to be  $1.05\text{m}$  with due clearance on either side.

### Thickness of jet (S<sub>0</sub>):

Thickness of the jet is calculated by dividing the jet area by runner breadth, as follows:

$$S_0 = 0.2 D_1$$

The jet thick thus calculated is  $5.8\text{ cm}$ .

### Spacing of blades in the runner:

$s_1 = K D_1$ , which comes out to be  $2.5\text{ cm}$ .

$$t = \frac{s_1}{\sin \beta_1}$$

$t = 2/\sin 30^\circ = 5.05\text{cm}$

### Number of blades:

$n = \frac{\pi D_1}{t}$ , which gives number of blades to be 18.

### Radial rim width:

$a = 0.17 D_1$  i.e.,  $= 4.93\text{cm}$

### Inner diameter of the runner:

$D_2 = D_1 - 2a$ , i.e.,  $= 19.14\text{cm}$

### Radius of blades curvature:

$\rho = 0.326 r_1$ , i.e.,  $= 4.73\text{cm}$

### Distance of jet from centre of shaft:

$y_1 = (0.1986 - 0.945k) D_1$ , i.e.,  $= 3.36\text{cm}$

### Distance of jet from inner periphery of the runner:

$y_2 = (0.1314 - 0.945k) D_1$ , i.e.,  $= 1.42\text{cm}$

### Angles:

#### Angle of Attack ( $\alpha_1$ ):

$$\eta = \frac{2C^2 u_1 (1 + \frac{\psi \cos \beta_2}{\cos \beta_1}) (\cos \alpha_1 - \frac{u_1}{V_1})}{V_1}$$

The above equation for turbine efficiency implies that  $\alpha_1$  should be decreased in order to increase efficiency. The angle of attack may be decreased to  $16^\circ$  with convenience of construction therefore an angle of attack of  $16^\circ$  is chosen.

Angle between relative velocity of entering water jet and outer runner periphery ( $\beta_1$ ):

Since,  $u_1 = 0.5(V_1 \cos \alpha_1)$

From the velocity triangle (Fig. 1):

$$\tan \beta_1 = 2 \tan \alpha_1$$

putting  $\alpha_1 = 16^\circ$  gives  $\beta_1 = 30^\circ$ .

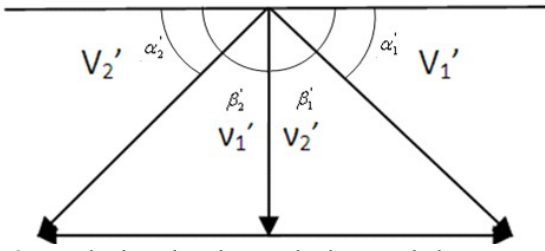


Fig. 2: Velocity triangle to calculate angle between runner periphery and relative velocity

**First Stage Blade Exit Angle ( $\beta_2'$ ):**

For a perfect radial flow  $\beta_2'$  should be equal to  $90^\circ$ . On account of the difference between the height of first stage exit and the second stage inlet the two velocities might differ i.e.,

$$V_1' = \sqrt{2gh_2 + V_2'^2}$$

It is recommended that to increase the blade exit angle above  $90^\circ$  in order to prevent shock losses. Shock losses arise when the relative velocities of the first stage exit and second stage entrance are not concurrent. This concept is elaborated in Fig 3.

**Runner material:**

Carbon Steel Castings are commonly used for turbine runners. ASTM A216 castings are of slightly higher strength than the more commonly used ASTM A27 material. ASTM A216 material is therefore used where increased mechanical strength is required. Keeping in view the unusually high flow-rate at the site under consideration, ASTM A216 is selected as the material for runner construction. Besides strength, it also provides relatively better resistance against corrosion and sand erosion.

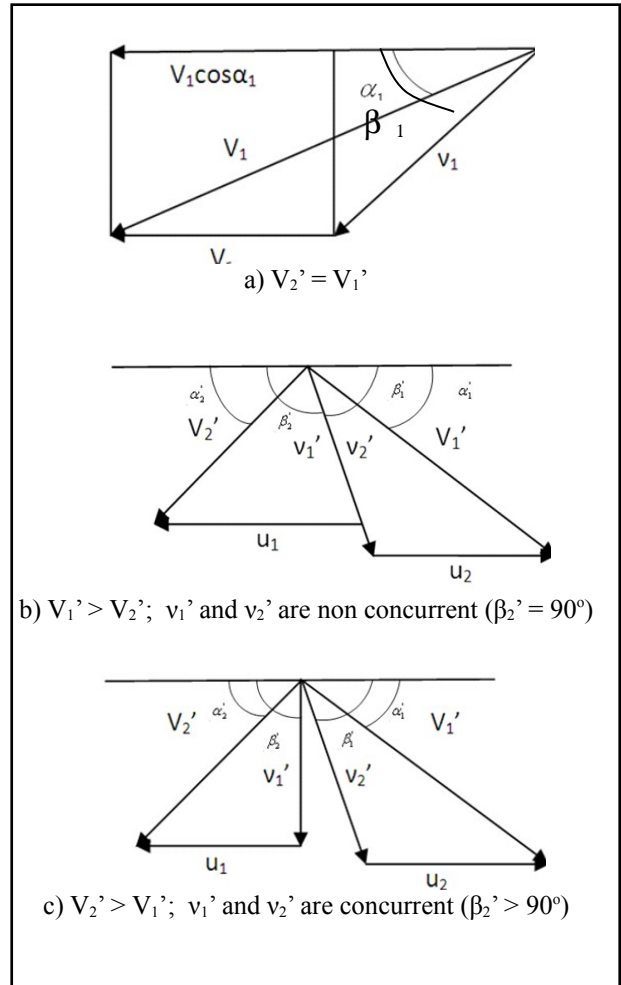


Fig 3: Various possibilities of relative velocities of first and second stages

**Penstock Design:**

The penstock pipe transports water under pressure from the forebay tank to the turbine, where the potential energy of the water is converted into kinetic energy in order to rotate the turbine. The penstock is often the most expensive item in the project budget – as much as 40 percent is not uncommon in most of the installations. It is therefore worthwhile to optimize its design in order to minimize its cost. The choice of size and type of penstock depends on several factors. Basically, the trade-off is between head loss and capital cost.

Head loss due to friction in the penstock pipe depends principally on the velocity of the water, the roughness of the pipe wall and the length and diameter of the pipe. The losses decrease substantially with increased pipe diameter. Conversely, pipe costs increase steeply with diameter. Therefore, a compromise between cost and performance is required. The Manning equation can be used for the calculation of the penstock diameter:

$$\frac{h_f}{L} = \frac{10.3n^2 Q^2}{d_1^{5.333}}$$

If pipe losses (due to friction and turbulence) are assumed to be 4% of the net head, then the equation comes out to be:

$$d_1 = 2.69 \left( \frac{n^2 Q^2 L}{H} \right)^{0.1875}$$

Taking length, L = 2m, d<sub>1</sub> is thus calculated to be = 0.68m.

The next step is to select a penstock material. The main characteristics considered in selection of material for penstock construction are :

- Young's Modulus of Elasticity
- Coefficient of linear expansion
- Ultimate Tensile strength
- Hazen William's coefficient

The properties of materials typically considered are tabulated in Table 2.

Material	Young's Modulus of Elasticity	Co-efficient of linear expansion	Ultimate Tensile strength	Hazen William's Coefficient
Welded Steel	206	12	400	0.012
Poly-ethylene	0.55	140	5	0.009
PVC	2.75	54	13	0.009
Cast Iron	78.5	10	140	0.014
Ductile Iron	16.7	11	340	0.015

The preference matrix analysis is then performed to select the most appropriate material, the material with the highest weighted score is selected. The results are tabulated in Table 3 below.

Table 3a - Welded Steel

Criterion	Weight	Score	WeightxScore
Young's Modulus	15	1	15

Criterion	Weight	Score	WeightxScore
of Elasticity			
Coefficient of linear expansion	15	0.833	12.5
Ultimate Tensile strength	40	1	40
Hazen Williams coefficient	30	0.75	22.5
Weighted Score			89.9

Table 3b – Polyethylene

Criterion	Weight	Score	WeightxScore
Young's Modulus of Elasticity	15	0.002	0.03
Coefficient of linear expansion	15	0.07	1.05
Ultimate Tensile strength	40	0.125	5
Hazen Williams coefficient	30	1	30
Weighted Score			36.1

Table 3c – PolyVinylChloride(PVC)

Criterion	Weight	Score	WeightxScore
Young's Modulus of Elasticity	15	0.011	0.165
Coefficient of linear expansion	15	0.185	2.775
Ultimate Tensile strength	40	0.0325	1.3
Hazen Williams coefficient	30	1	30
Weighted Score			34.2

Table 3d – Cast Iron

Criterion	Weight	Score	WeightxScore
Young's Modulus of Elasticity	15	0.381	5.7
Coefficient of linear expansion	15	1	15
Ultimate Tensile strength	40	0.35	14
Hazen Williams coefficient	30	0.64	19.2
Weighted Score			53.9

Table 3e – Ductile Iron

Criterion	Weight	Score	WeightxScore
Young's Modulus of Elasticity	15	0.081	1.22
Coefficient of linear expansion	15	0.91	13.65
Ultimate Tensile strength	40	0.85	34

Hazen coefficient	Williams	30	0.6	18
Weighted Score				66.87

Based on these calculations, the welded steel has the highest weighted score and is therefore selected as the material for the penstock construction.

## CONCLUSION

A typical site has been selected for installing a micro-hydro power station. In the past a pump as Turbine has been installed at that site and efforts are underway to install another turbine at the spillway. A cross flow turbine was found suitable for the site conditions and complete design of such a turbine has been presented in this paper. In this regard turbine runner diameter, runner tangential velocity and angular velocities have been determined. The runner outer diameter and breadth are also determined. The design also includes the radial rim width, radius of curvature of the blades and number of blades. The jet diameter, angle of attack and the distance of nozzle from the runner have also been calculated in addition to runner material selection. Finally penstock design and material selection have also been discussed to complete the cross flow turbine design. The turbine has a theoretical power generation potential of about 50 kW.

## REFERENCES

- [1] J.A. Chattha, M.S. Khan, "Experimental study to test an axial flow pump as a turbine and development of performance characteristics for micro-hydro power plant" Proceedings of the ASME Power 07 Conference July 17-19, 2007, San Antonio, Texas, USA
- [2] J.A. Chattha, M.S. Khan and A. Haque, "Micro-hydro power systems: Current status and future research in Pakistan" Proceedings of the ASME Power 09 Conference July 21-23, 2009, Albuquerque, New Mexico, USA
- [3] OSSBERGER turbine.

<http://www.ossberger.de/cms/en/hydro/the-ossberger-turbine/#c152>

- [4] Khosrowpahan, S., "Experimental Study of the Crossflow Turbine", Ph.D. Dissertation, Colorado State University, Fort Collins, CO, 1984.
- [5] Nakase, Y., Fukutomi, J., Wantanabe, T., Suessugu, T., and Kubota, T., "A study of Crossflow Turbine", Small Hydro Power Fluid Machinery, p. 13-18, 1982.
- [6] Akerkar, B. P., "A Study of the Performance of the Crossflow Turbine", M.S. thesis, Clemson University, Clemson, SC, 1989.
- [7] Fiuzat, A.A., and Akerkar B.P., "The Use of Interior Guide Tube in Crossflow Turbines", International Conference on Hydropower; Waterpower 1989 . p. 1111-1119
- [8] Chappell, J. R., "Recent DOE-Sponsored Hydropower Engineering Research", Report No. ECG-M-02983, p6, 1983
- [9] Simpson, B. J., "Low Head, Micro-Hydro Demonstration Project, Coker Alabama, Final Report", Report No. DOE/R4 10233-TI, 1983
- [10] Hayati Olgun, "Effect of interior guide tubes in cross-flow turbine runner on turbine performance", International Journal of Energy Research, p 953-964, 2000 John Wiley & Sons
- [11] Hayati Olgun, "Investigation of the Performance of a Cross-Flow Turbine", International Journal of Energy Research, pp 953-964, 1998 John Wiley & Sons
- [12] Durgin W.W and Fay W.K, "Some Fluid Flow Characteristics of a Cross-Flow Type Hydraulic Turbine" Small Hydro Power Fluid Machinery, 1984, p77-83. The Winter Annual meeting of ASME, New Orleans, L.A, December 9-14, 1984
- [13] Nadim M. Aziz and V. R. Desai, "An Experimental Study of the Effect of Some Design Parameters in Cross-Flow Turbine Efficiency", Engineering Report, Department of Civil Engineering, Clemson University, 1991.
- [14] Thapar, O.D., and Albertson, M.L., "Ultra Low Head Small Hydro Power System Technology for Economic Development", Waterpower 1985
- [15] Mockmore C. A., and Merryfield, F., "The Banki water turbine." Engineering experimental station bulletin series No. 25, February 1949, p 22

## APPENDIX B1

### SOFTWARE CODE

#### 1. Input Form Code

```
using System;

using System.Collections.Generic;

using System.ComponentModel;

using System.Data;

using System.Drawing;

using System.Linq;

using System.Text;

using System.Windows.Forms;

using System.Diagnostics;

namespace Micro_Hydro_Software_1._1

{

    public partial class Form1 : Form

    {

        Name.Result R = new Name.Result();

        public double AngleOfAttack = 0.384;

        public double GeneratorRPM = 1550;

        public double DiameterRatio = 0.7;

        public double BladeExitAngle = 0.9599;

        public double FrictionFactor = 0.15;

        public Form1()

        {

            InitializeComponent();

        }

        private void Calculate_Click(object sender, EventArgs e)

        {
```



```

//Micro_Hydro_Software_1._1.Result R = new Result();

//float GrossHead = float.Parse(GrossHeadText.Text.ToString());

//float PES = float.Parse(ChannelAreaText.Text.ToString());

//float h = float.Parse(Math.Pow(GrossHead, 0.5).ToString());

//float result = (1142 * h) / PES;

    try

        {R.Headloss = Math.Round( 0.04 * double.Parse(GrossHeadText.Text.ToString()),2);

R.NetHead = Math.Round( double.Parse(GrossHeadText.Text.ToString()) -R.Headloss, 2);

    double Variable1 = 2 * 9.81 * R.NetHead;

    double Variable2 = 0.98 * (Math.Sqrt(Variable1));

    double Variable3 = 0.5 * Variable2 * Math.Cos(AngleOfAttack);

    double Variable4 = GeneratorRPM / double.Parse(SpeedRatioText.Text);

R.RunnerRPM = Math.Round(Variable4, 2);

R.OuterDiameter = Math.Round( (Variable3 * 60) / (Variable4 * Math.PI), 2);

R.InnerDiameter = Math.Round( R.OuterDiameter * DiameterRatio, 2);

R.WidthOfRunner = Math.Round(((2.6 * double.Parse(FlowRateText.Text)) /
(Math.Sqrt(R.NetHead) * R.OuterDiameter), 2);

R.ThicknessOfJet = Math.Round( 0.2 * R.OuterDiameter, 2);

R.RadialRimWidth = Math.Round( (R.OuterDiameter - R.InnerDiameter) / 2, 2);

    double BladeInletAngle = Math.Atan(2 * Math.Tan(AngleOfAttack));

R.BladeInletAngle = Math.Round( (BladeInletAngle * 180) / Math.PI, 2);

R.SpacingOfBlades = Math.Round( (0.087 * R.OuterDiameter) / Math.Sin(BladeInletAngle), 2);

R.NoOfBlades = Math.Round( (Math.PI * R.OuterDiameter) / R.SpacingOfBlades, 2);

    double Variable5 = (R.OuterDiameter * (1 - Math.Pow(DiameterRatio, 2))) / 4;

    double Variable6 = (Math.Cos(BladeInletAngle) - DiameterRatio *
Math.Cos(BladeExitAngle));

R.RadiusOfBladeCurvature = Math.Round( Variable5 / Variable6, 2);

```

```

double Variable7 = 41280 * double.Parse(FlowRateText.Text);

double Variable8 = double.Parse(GeneratorRPMText.Text) * Math.PI *
((Math.Pow(R.OuterDiameter, 2) - Math.Pow(R.InnerDiameter, 2)));

R.NozzleWidth = Math.Round( Variable7 / Variable8, 2);

        double Variable9 = (4.66 * Math.Pow(FrictionFactor, 2) *
        double.Parse(LengthOfPenstockText.Text) *
        Math.Pow(double.Parse(FlowRateText.Text), 2)) / R.Headloss;

R.PenstockDiameter = Math.Round( Math.Pow(Variable9, 0.1876), 2);

R.ExpectedPowerOutput = Math.Round ((double.Parse(ExpectedEfficiencyText.Text) * 999 *
9.81 * R.NetHead * double.Parse(FlowRateText.Text)) / 1000, 2);

    }

    catch (Exception exp)

    {

        //MessageBox.Show("Please Enter All Values");

    }

    Results resultPage = new Results(R);

    resultPage.Show();

}

private void HelpButton_Click(object sender, EventArgs e)

{

Process.Start(@"D:\Vs Projects\Micro Hydro Software 1.1\Micro Hydro Software
1.1\NewFolder1\Help_File!.pdf");

}

private void Form1_Load(object sender, EventArgs e)

{

}

}

}

```

## 2. Results Page Code

```
using System;

using System.Collections.Generic;

using System.ComponentModel;

using System.Data;

using System.Drawing;

using System.Linq;

using System.Text;

using System.Windows.Forms;

namespace Micro_Hydro_Software_1._1

{

    public partial class Results : Form

    {

        Name.Result RR = new Name.Result();

public Results()

    {

        InitializeComponent();

    }

    public Results(Name.Result R)

    {

        InitializeComponent();

        RR = R;

        HeadLossLabel.Text = R.Headloss.ToString() + " m";

        NetHeadLabel.Text = R.NetHead.ToString() + " m";

        RunnerRPMLabel.Text = R.RunnerRPM.ToString();

        OuterDiameterLabel.Text = R.OuterDiameter.ToString() + " m";

        InnerDiameterOfRunnerLabel.Text = R.InnerDiameter.ToString() + " m";

        WidthOfRunnerLabel.Text = R.WidthOfRunner.ToString() + " m";

        ThicknessOfJetLabel.Text = R.ThicknessOfJet.ToString() + " m";

    }

}

}
```

```

RadialRimWidthLabel.Text = R.RadialRimWidth.ToString() + " m";
BladeInletAngleLabel.Text = R.BladeInletAngle.ToString() + " Degrees";
SpacingOfBlades.Text = R.SpacingOfBlades.ToString() + " m";
NoOfBladesLabel.Text = R.NoOfBlades.ToString();
RadiusOfBladeCurvatureLabel.Text = R.RadiusOfBladeCurvature.ToString() + " m";
NozzleWidthLabel.Text = R.NozzleWidth.ToString() + " m";
PenstockDiameterLabel.Text = R.PenstockDiameter.ToString() + " m";
ExpectedPowerOutputLabel.Text = R.ExpectedPowerOutput.ToString() + " kW";
}
private void Convert_Click(object sender, EventArgs e)
{
    if (Convert.Text == "Convert to English Units")
    {
        Convert.Text = "Convert to SI Units";

        HeadLossLabel.Text = Math.Round((RR.Headloss * 39.3700787), 2).ToString() + "
inches";

        NetHeadLabel.Text = Math.Round((RR.NetHead * 39.3700787), 2).ToString() + "
inches";

        OuterDiameterLabel.Text = Math.Round((RR.OuterDiameter * 39.3700787),
2).ToString() + " inches";

        InnerDiameterOfRunnerLabel.Text = Math.Round((RR.InnerDiameter * 39.3700787),
2).ToString() + " inches";

        WidthOfRunnerLabel.Text = Math.Round((RR.WidthOfRunner * 39.3700787),
2).ToString() + " inches";

        ThicknessOfJetLabel.Text = Math.Round((RR.ThicknessOfJet * 39.3700787),
2).ToString() + " inches";

        RadialRimWidthLabel.Text = Math.Round((RR.RadialRimWidth * 39.3700787),
2).ToString() + " inches";

```

```

        SpacingOfBlades.Text = Math.Round((RR.SpacingOfBlades * 39.3700787),
2).ToString() + " inches";

        RadiusOfBladeCurvatureLabel.Text = Math.Round((RR.RadiusOfBladeCurvature *
39.3700787), 2).ToString() + " inches";

        NozzleWidthLabel.Text = Math.Round((RR.NozzleWidth * 39.3700787),
2).ToString() + " inches";

        PenstockDiameterLabel.Text = Math.Round((RR.PenstockDiameter * 39.3700787),
2).ToString() + " inches";
    }
else
{
    Convert.Text = "Convert to English Units";
    HeadLossLabel.Text = RR.Headloss.ToString() + " m";
    NetHeadLabel.Text = RR.NetHead.ToString() + " m";
    OuterDiameterLabel.Text = RR.OuterDiameter.ToString() + " m";
    InnerDiameterOfRunnerLabel.Text = RR.InnerDiameter.ToString() + " m";
    WidthOfRunnerLabel.Text = RR.WidthOfRunner.ToString() + " m";
    ThicknessOfJetLabel.Text = RR.ThicknessOfJet.ToString() + " m";
    RadialRimWidthLabel.Text = RR.RadialRimWidth.ToString() + " m";
    SpacingOfBlades.Text = RR.SpacingOfBlades.ToString() + " m";
    RadiusOfBladeCurvatureLabel.Text = RR.RadiusOfBladeCurvature.ToString() + " m";
    NozzleWidthLabel.Text = RR.NozzleWidth.ToString() + " m";
    PenstockDiameterLabel.Text = RR.PenstockDiameter.ToString() + " m";
}
}
}
}

```

### 3. Main Program Code

```
using System;

using System.Collections.Generic;

using System.Linq;

using System.Windows.Forms;

namespace Micro_Hydro_Software_1._1
{
    static class Program
    {
        /// <summary>
        /// The main entry point for the application.
        /// </summary>
        [STAThread]
        static void Main()
        {
            Application.EnableVisualStyles();
            Application.SetCompatibleTextRenderingDefault(false);
            Application.Run(new Form1());
        }
    }
}
```



# APPENDIX B2

SOFTWARE HELP FILE



<b>PARAMETER</b>	<b>DESCRIPTION</b>	<b>ILLUSTRATION</b>
HEAD LOSS	A measure of the reduction in the total head because of the friction between the fluid and the walls of the pipe.	
NET HEAD	The difference between the actual (Gross) head and the Head Loss	
OUTER DIAMETER	The Outer Diameter of the Runner Cross-Section	
INNER DIAMETER	The Inner Diameter of the Runner Cross-Section	
RUNNER RPM	The Angular Velocity of the Runner	
THICKNESS OF JET	The thickness of the water jet striking the nozzle	
RADIAL RIM WIDTH	The difference between the outer and inner radii	
ANGLE OF ATTACK	The angle between the Outer Periphery of the Runner and the Absolute Velocity of Entering Water Jet at the 1 <sup>st</sup> Stage	
RADIUS OF BLADE CURVATURE	The Radius of the Curvature of the Blade with respect to an imaginary circle drawn through the blade	
SPACING OF BLADES	The distance between two successive blades	
BLADE INLET ANGLE	Angle between the Relative Velocity of Entering Water Jet and Outer Runner Periphery	
BLADE EXIT ANGLE	Angle between Relative Velocity of Exiting Water Jet and Inner Runner Periphery	
NOZZLE ENTRY ARC	The portion of the runner (in terms of angle) which is directly exposed to the water jet leaving the nozzle	
SPEED RATIO	The Ratio of the Speed of the Generator to the Speed of the Runner	
FRICTION FACTOR	A constant accounting for the friction losses in the pipe	
DIAMETER RATIO	The ratio of the inner to the outer Diameter	

